The Astronomical Journal, 165:240 (16pp), 2023 June https://doi.org/10.3847/1538-3881/acc9bf

H I 21 cm Extended Structures to the Northeast and Southwest of NGC 5595: VLA Observations of the Disk Galaxy Pair NGC 5595 and NGC 5597

J. Antonio Garcia-Barreto[1] and Emmanuel Momjian[2]
[1] Instituto de Astronomia, Universidad Nacional Autónoma de México, Apartado Postal 70-264, Ciudad de México 04150, México
j.antonio.garcia.barreto@astro.unam.mx
[2] National Radio Astronomy Observatory, P.V.D. Science Operations Center, P.O. Box O, Lopezville Road, Socorro, NM 87801-0387, USA
Received 2022 November 4; revised 2023 March 29; accepted 2023 March 31; published 2023 May 15

Abstract

We report VLA B-configuration observations of the H I 21 cm line on the close disk galaxy pair NGC 5595 and NGC 5597. At the angular resolution of the observations, $\sim 7\farcs1 \times 4\farcs2$, while most of the H I 21 cm in NGC 5595 and NGC 5597 has the same extent as the optical disk, we have detected for the first time extended structures (streamers) to the northeast (NE) and southwest (SW) of NGC 5595 with no counterparts in blue, red optical (continuum), 20 cm radio continuum, or Hα spectral line emission. One structure is extended by $\sim 45''$ to the NE with blueshifted velocities, and the other is extended by $\sim 20''$ to the SW with redshifted velocities with respect to the systemic velocity. No H I 21 cm emission is detected from the innermost central (nuclear) regions of either galaxy. Lower angular resolution H I 21 cm imaging indicates the nonexistence of any intergalactic hydrogen atomic H I 21 cm gas as tails or bridges between the two galaxies. Our new 20 cm radio continuum emission image of NGC 5597 shows a strong unresolved elongated structure in the central region, in the NE–SW direction, very similar to the spatial location of the innermost Hα spectral line emission. There is no 20 cm continuum emission from its northern spiral arm. In NGC 5595, the 20 cm radio continuum image shows no continuum emission from the NE or SW extended structures with H I 21 cm emission.

Unified Astronomy Thesaurus concepts: Galaxy interactions (600); Galaxy kinematics (602); Galaxy dynamics (591); Galaxy rotation curves (619); Galaxy tides (623)

1. Introduction

From the observational point of view, ongoing major and minor gravitational interactions of two or more disk galaxies show extended H I 21 cm cold gas structures of tidal origin, with M51 and NGC 5195 being one of the classic examples (Sancisi 1999).

The numerical simulations performed by Toomre & Toomre (1972) have convincingly shown that the gravitational interactions in very close pairs of disk galaxies in their late stages of merging cause stellar tails and bridges (e.g., M51 with NGC 5195, NGC 4038 with NGC 4039, and NGC 4676A with NGC 4676B, the Mice). They went even further and dared to raise the possibility that the innermost density-wave spiral pattern in galaxies such as M51 and NGC 7753 was indirectly caused by the recent external influences (see their Section VII, Subsection d, ending with the question, "*Et tu* M81?," referring to M81 with the close companion NGC 3077).

Since then, gravitational interaction between a close pair of disk galaxies has been recognized to be important in determining their gas kinematics, dynamics, star formation, central feeding of a massive black hole, and evolution in time (Mihos & Hernquist 1994, 1996).

Recent galaxy distribution surveys have confirmed that galaxies are found in a hierarchical structure of filaments and walls that surround large galaxy voids with 54% in the local universe concentrated in virialized clusters and groups and only 7% as isolated pairs of galaxies (Argudo-Fernandez et al. 2015). Galaxy pairs detected in the far-infrared by the Infrared Astronomical Satellite (IRAS) have a median separation of $20\,h^{-1}$ kpc, and pairs that are most likely close together in space have greater specific star formation rates (SSFRs; Geller et al. 2006). Using Hα line emission to estimate the star formation rate in major mergers[3] from 2409 galaxies reveals enhanced star formation in cases where the gravitational tidal force is relatively strong compared to the self-gravity of a galaxy (Woods & Geller 2007). These authors also found that for major mergers, there is a correlation between SSFR and separation (on the plane of the sky), ΔD, in such a way that the smaller the ΔD, the higher the SSFR (Woods & Geller 2007).

Radio continuum observations at $\lambda \sim 11$, 6, and 3.7 cm of disk–disk pairs from the Catalog of Isolated Pairs of Galaxies (Karachentsev 1972) revealed a correlation between physical separation and radio emission, with close pairs being radio-emitting sources at more than twice the number of more widely spaced pairs (Stocke 1978; Stocke et al. 1978). Westerbork radio interferometer continuum observations at 1.415 GHz have shown that the radio power of the central sources in pairs of galaxies is, on average, four times higher than in isolated disk galaxies (Hummel 1981; Hummel et al. 1987). Furthermore, Karl G. Jansky Very Large Array (VLA) radio continuum observations at 1.46 and 4.88 GHz of 60 interacting galaxies have shown that, on average, the radio power of the central radio sources is about a factor of 5 higher than in isolated galaxies, and that the radio power of central radio sources in barred disk galaxies is a factor of 5 higher than in nonbarred disk galaxies (Hummel et al. 1987, 1990).

[3] Major mergers have been defined as pairs of galaxies whose differences in apparent magnitude are less than 2, $\Delta m \leqslant 2$; minor mergers, on the contrary, are pairs of galaxies whose differences in apparent magnitude are more than 2, $\Delta m \geqslant 2$ (Woods & Geller 2007).

What Toomre & Toomre (1972) did not explicitly state was that narrow and long tails and bridges of cold H I 21 cm gas are also caused by gravitational interaction of close pairs of disk galaxies. Indeed, three of the most beautiful examples of H I 21 cm imaging of interactions in a system of galaxies are (i) NGC 5194 (M51, Sbc(s)I-II) with its southeast (SE) long tail and its companion NGC 5195 (SB01 pec; Davies 1974; Haynes et al. 1978; Appleton et al. 1986; Rots et al. 1990); (ii) the M81 (Sb(r)I-II)–M82 (amorphous) and NGC 3077 (Irr) system with cold atomic hydrogen gas structures from a northern tidal bridge between M82 and NGC 3077, a southern tidal bridge between NGC 3077 and M81, and the structure between M81 and M82 (Cottrell 1976; van der Hulst 1979; Yun et al. 1993, 1994); and (iii) NGC 4038/4039, the Antennae (NGC 4038 SB,(s)mpec and NGC 4039 SAB(s)mpec; van der Hulst 1979; Gordon et al. 2001; Hibbard et al. 2001).

One such nearby disk galaxy pair system is NGC 5595 and NGC 5597. For this system, we adopt a Hubble (spectroscopic) distance of $D_{\rm pair} = 38.6$ Mpc (Tully 1988), giving an approximate angular-to-linear scale of $1\farcs0, \sim 187.14$ pc. The projected separation (on the plane of the sky) between the two galaxies is $\sim 3\farcm97$, or $\sim$45 kpc. Our analysis of the H I 21 cm gas emission, rotation curve, and angular velocity in NGC 5597 using data obtained with the VLA[4] in B-configuration and the subsequent estimation of the angular velocity pattern of its stellar bar have already been reported (Garcia-Barreto & Momjian 2022).

Since NGC 5595 and NGC 5597 are so close on the plane of the sky, a single VLA pointing (primary beam full width at half-power, $\theta_{\rm HPBW} = 30'$ at 1.4 GHz) was required to observe the H I 21 cm emission from the disk galaxy pair system. Therefore, here we report the overall H I 21 cm kinematics and dynamics of each disk galaxy and their close environment.

Galaxy NGC 5597 was originally chosen from a list of 56 nearby, bright, barred galaxies with IRAS 60 μm flux densities greater than 5 Jy (Garcia-Barreto et al. 1996) and colors indicative of circumnuclear star formation (Helou et al. 1985). Its IRAS flux densities are $f_{60\mu{\rm m}} \sim 8.7$ and $f_{100\mu{\rm m}} \sim 15.32$ Jy with $T_{\rm dust} \sim 36$ K. In 1996, we were only aware that NGC 5597 was part of Tully's group $41 + 15 + 15$. Later, we carried out the study of companions for the same set of nearby bright barred galaxies utilizing the NASA/IPAC Extragalactic Database (NED)[5] and found that NGC 5597 has only one nearby disk galaxy companion, namely, NGC 5595 (Garcia-Barreto et al. 2003). Based on their projected spatial proximity ($\Delta D_{12}/(d_1 + d_2) \leqslant 2$; Zwicky 1956; Karachentsev 1972, 1981) and very similar spectroscopic H I 21 cm systemic velocities ($\Delta V \leqslant 5$ km s^{-1}), NGC 5597 forms an isolated, gravitationally bound pair with the disk galaxy NGC 5595 (Sc).

There is also growing evidence of weak nuclear activity in normal disk galaxies with and without a prominent stellar bar, with observational detection of nuclear low-velocity bipolar outflows in Hα, e.g., M81 (Goad 1976), NGC 1068 (Ulvestad et al. 1987), M51 (Ford et al. 1985; Cecil 1988; Crane & van der Hulst 1992; Scoville et al. 1998), NGC 3079 (Veilleux et al. 1994), M101 (Moody et al. 1995), NGC 3367 (Garcia-Barreto et al. 1998, 2002), and NGC 1415 (Garcia-Barreto et al. 2019), suggesting that they represent the low end of the scale for nuclear activity after quasars, BL Lac objects, radio galaxies, and Seyfert galaxies. All such phenomena have an origin in events occurring around central massive black holes, with the level of the activity being governed by the gas supply to fuel these central engines (Norman & Silk 1983). Similar physical processes have also been observed in NGC 3367 (Garcia-Barreto et al. 1998, 2002, 2005; Hernández-Toledo et al. 2011).

In this paper, we present VLA B-configuration observations of atomic hydrogen, H I 21 cm, cold gas emission at an angular resolution of $7\farcs1 \times 4\farcs2$ at P.A. $\sim -10°$ east of north (E of N; or about 1.33×0.78 kpc in linear size), as well as new 20 cm radio continuum emission from the disk galaxy pair NGC 5595 and NGC 5597. We have imaged the global H I 21 cm emission from this galaxy pair to probe the internal kinematics and investigate the existence of any large-scale gas structure between them. We have also made 20 cm radio continuum emission images for both disk galaxies. For the barred galaxy NGC 5597, we compare its 20 cm continuum emission with previously published Hα spectral line emission and blue optical (broadband continuum from a 103aO glass plate) spatial distribution, especially in the inner $30\farcs0$. This work is organized as follows. Section 2 presents the observations and data reduction. Section 3 presents the disk galaxy system as an isolated gravitationally bound pair. Section 4 presents some properties of NGC 5597 as an SBc disk galaxy. Section 5 presents some properties of NGC 5595 as an Sc disk galaxy, Section 6 presents the H I 21 cm features in the field of the disk galaxy pair NGC 5595 and NGC 5597, and, finally, Section 7 presents the summary and conclusions.

2. Observations and Data Reduction

Two-dimensional velocity fields for the H I 21 cm emission from the disk galaxy pair NGC 5595 and NGC 5597 were obtained using the VLA in its B-configuration on 2019 June 6, 7, 11, 16, 18, and 22. On each day, the total observing time was about 1.5 hr and included 100 minutes of on-source time, as well as overhead to observe the flux density scale/bandpass calibrator 3C 286 and the complex gain calibrator J1448−1620. The VLA system was tuned to the rest frequency of the H I 21 cm line, $\nu_{\rm rest} = 1{,}420{,}405.752$ kHz, redshifted to a mean heliocentric velocity of $v_{\rm pair} = 2700$ km s^{-1} for the galaxy pair system. Table 1 lists the coordinates, Hubble type, distance, and systemic H I velocities of NGC 5595 and NGC 5597. Furthermore, because these two galaxies are separated by only $\leqslant 4'$ on the plane of the sky and are well within the primary beam of the VLA antennas ($\theta_{\rm HPBW} = 30'$ at 1.4 GHz), the pointing center of the observations was chosen to be midway between the two disk galaxies: $\alpha_{\rm mid} = 14^{\rm h}\,24^{\rm m}\,21\farcs0$, $\delta_{\rm mid} = -16°\,44'\,45\farcs0$.

The observations utilized one of the 1 GHz wide 8-bit sampler pairs of the VLA, namely, A0/C0, and the Wideband Interferometric Digital ARchitecture correlator was configured to deliver a single 4 MHz wide subband with 256 spectral channels, resulting in a channel spacing of 15.625 kHz, or 3.3 km s^{-1}. This subband spans a velocity range of $\Delta V \sim 843$ km s^{-1}, which is sufficient to cover the full width at zero intensity of the H I emission from both NGC 5595 and NGC 5597 and provide line-free channels for continuum subtraction.

We used the Common Astronomy Software Applications (CASA) for the flux density scale, bandpass, complex gain calibration, and continuum subtraction, as well as deconvolution and imaging. The Astronomical Image Processing System

[4] The National Radio Astronomy Observatory is a facility of the National Science Foundation operated under cooperative agreement by Associated Universities, Inc.

[5] The NED is operated by the Jet Propulsion Laboratory, California Institute of Technology, under contract with the National Aeronautics and Space Administration.

Table 1
NGC 5595–NGC 5597 Pair of Disk Galaxies: Coordinates, Hubble Type, Distance, and Systemic H I Velocity

Galaxy Name	α(J2000) hh mm ss	δ(J2000) deg arcmin arcsec	Reference	RSA Type	NED Type	Distance Mpc	Reference	V(H I)$_{sys}$ km s^{-1}	Reference
(1)	(2)	(3)	(4)	(5)	(6)	(7)	(8)	(9)	(10)
NGC 5595	14 24 13.3	−16 43 21.6	1	Sc(s) II	SAB(rs)c	38.6	2	2697	3
NGC 5597	14 24 27.49	−16 45 45.9	1	SBc(s) II	SAB(rs)b	38.6	2	2698	3

Note. (1) Diaz-Hernández et al. (2009); (2) Tully (1988); (3) Paturel et al. (2003).

(AIPS) was utilized for the spectral and kinematics analysis and the presentation and overlay of 20 cm continuum, Hα, and optical 103aO images.

The data set of each session was calibrated independently, and image cubes were made to determine the line-free channels for continuum subtraction. Line+continuum emission from NGC 5597 was confined between channels 81 and 200, and that from NGC 5595 was confined between channels 81 and 197. The continuum emission was subtracted from the line +continuum data in the *uv* plane. The H I image cube was then produced by combining the data from all of the sessions using a cell size of 1.″0 and Briggs weighting with robust = 0.8. The resulting synthesized beam was ∼7.″1 × 4.″2 (1.33 × 0.78 kpc^2) at FWHM with P.A. ∼ −10° E of N. This image cube was imported to AIPS for further analysis. In there, moments 0, 1, and 2 were made using a flux density cutoff of 2.5σ, with 1σ ∼ 450 μJy beam^{-1} channel^{-1}. The H I line-free 20 cm continuum emission, using the channel ranges 45–75 and 222–240 from all of the sessions, was also imaged in CASA using robust = 0. The resulting synthesized beam (FWHM) was ∼6.″1 × 3.″7 at P.A. ∼ −8° E of N, and the rms noise was 1σ, ∼167.4 μJy beam^{-1}.

To search for extended H I 21 cm cold atomic gas between NGC 5595 and NGC 5597, we have also made a low-resolution image cube using a *u*, *v* range restricted between zero and 5 kλ. This resulted in a synthesized beam (FWHM) of ∼30.″7 × 28.″8 at P.A. ∼ +50° E of N, corresponding to a linear resolution of ∼5.4 × 5.7 kpc^2.

3. Gravitationally Bound Isolated Pair: NGC 5597–NGC 5595

The disk galaxies NGC 5595 and NGC 5597 are in the Southern Virgo–Libra cloud of galaxies, Tully's group 41–14 (+14), with a very low galaxy volume density of only 0.16 galaxies Mpc^{-3}; see their spatial location at galactic coordinates $l^{II} \sim 332°.8, b^{II} \sim +40.7$ in Plates 1 and 5 of Tully & Fischer (1987) and α and δ in Figure 2 of Tammann (1985).

These two galaxies are separated by $\Delta\alpha \sim 13^s.54$, $\Delta\delta \sim 138''$, or $D_{12} \sim 3.''97$ on the plane of the sky. The diameters of NGC 5597 and NGC 5595 are $d_1 \sim 1.''87$ and $d_2 \sim 1.''6$, respectively. Furthermore, these two galaxies have very similar spectroscopic H I 21 cm systemic velocities ($\Delta V < 5$ km s^{-1}). Thus, they indeed satisfy Holmberg's spatial and velocity difference criteria $\Delta D_{12}/(d_1 + d_2) \ll 2$ (Zwicky 1956; Karachentsev 1972, 1981), indicating that NGC 5597 forms an isolated, gravitationally bound pair with the disk galaxy NGC 5595 (Sc).

Figure 1 shows a reproduction of the optical blue continuum 103aO emission from the disk galaxy pair NGC 5597 (SE) and NGC 5595 (northwest; NW) in gray scale in relative units taken with the OAN-SPM 2.1 m optical telescope in Mexico (Diaz-Hernández et al. 2009). In this blue optical continuum image, there are no bridges or structures connecting the two galaxies. In Section 5, it will be shown that there are H I 21 cm extended cold gas structures to the northeast (NE) and southwest (SW) of NGC 5595.

4. NGC 5597: A Late-type Barred Disk Galaxy

Object NGC 5597 is a bright ($m_B \sim 12.57$) disk galaxy classified as SBc(s) II (Sandage & Tammann 1981) and as SAB (s)cd in NED. Table 2 lists the spatial positions of its nucleus estimated from observations at different wavelengths, and Table 4 gives its basic properties.

Figure 2 shows a reproduction of the red optical (filter *I* 8040 Å) of the disk galaxy NGC 5597.[6] Both images of NGC 5597 in Figures 1 and 2 show a central elongated structure about $2a \sim 28.''3$ by $2b \sim 14''$ at P.A. ∼ 52° that we interpret as the boxy stellar bar and have estimated its angular velocity pattern (Ω_{bar}; Garcia-Barreto & Momjian 2022).

Additionally, as seen in the SE galaxy in Figure 1, and more specifically in Figure 2, there are at least four narrow and curved structures as spiral arms outside the central region of NGC 5597 (labeled 1–4 in Figure 2). The first structure (1) starts from the NE half of the stellar bar and extends to the SE, the second structure (2) starts from the SW of the S half of the stellar bar and extends further to the SW, and the third structure (3) starts from the NW of the S half of the boxy bar and extends further NW, joining the outer fourth structure.

The fourth structure (4) seems to start from the SW of the disk and continues counterclockwise to the N, NE, and SE just parallel to the outside of the first structure. A plausible interpretation of the N optical spiral arm in NGC 5597 would be that it is a spiral arm near an outer ultraharmonic resonance (UHM),[7] $m = 4$ (Contopoulos et al. 1989).

Figure 3 (left) shows our VLA B-configuration H I 21 cm spectrum for NGC 5597. Its overall shape is similar only to the previous Nançay spectrum because it has the approximate E–W angular resolution to isolate the emission from NGC 5597 (Paturel et al. 2003). The full width of the H I emission line at 20% of the

[6] The red optical image has not been calibrated in flux density scale; therefore, the contours are proportional to the rms noise in relative units.

[7] For a star (gas cloud) in an axisymmetric gravitational potential of a disk galaxy, Φ_{disk}, in addition to a weak nonaxisymmetric gravitational potential, Φ_{bar}, where $\Phi_{bar} << \Phi_{disk}$, its orbit can be represented as a superposition of the circular motion of a guiding center and small radial oscillations around this guiding center. In cylindrical coordinates with $z = 0$, the stellar bar gravitational potential may be expressed as $\Phi_{bar}(R, \varphi, z = 0) = \Phi_b\, cos(m\varphi)$. The equation of motion of a star (gas cloud) is given by the equation of motion of a harmonic oscillator of natural frequency $\kappa(R)$ that is driven at a frequency $m(\Omega_{star,gascloud} - \Omega_{bar})$. The solution of the radial motion becomes singular at different values of the guiding center. At the corotation radius, $\Omega_{star,gascloud} = \Omega_{bar}$. At other radii, $m(\Omega_{star,gascloud} - \Omega_{bar}) = \pm\kappa$; for $m = 2$, the plus and minus signs denote the so-called inner and outer Lindblad resonances. When $m = 4$ or 6, they denote the radii of the so-called UHMs; in particular, when $m = 4$, the minus sign denotes the outer UHM (Binney & Tremaine 1987; Contopoulos 1988; Contopoulos et al. 1989; Athanassoula 1992).

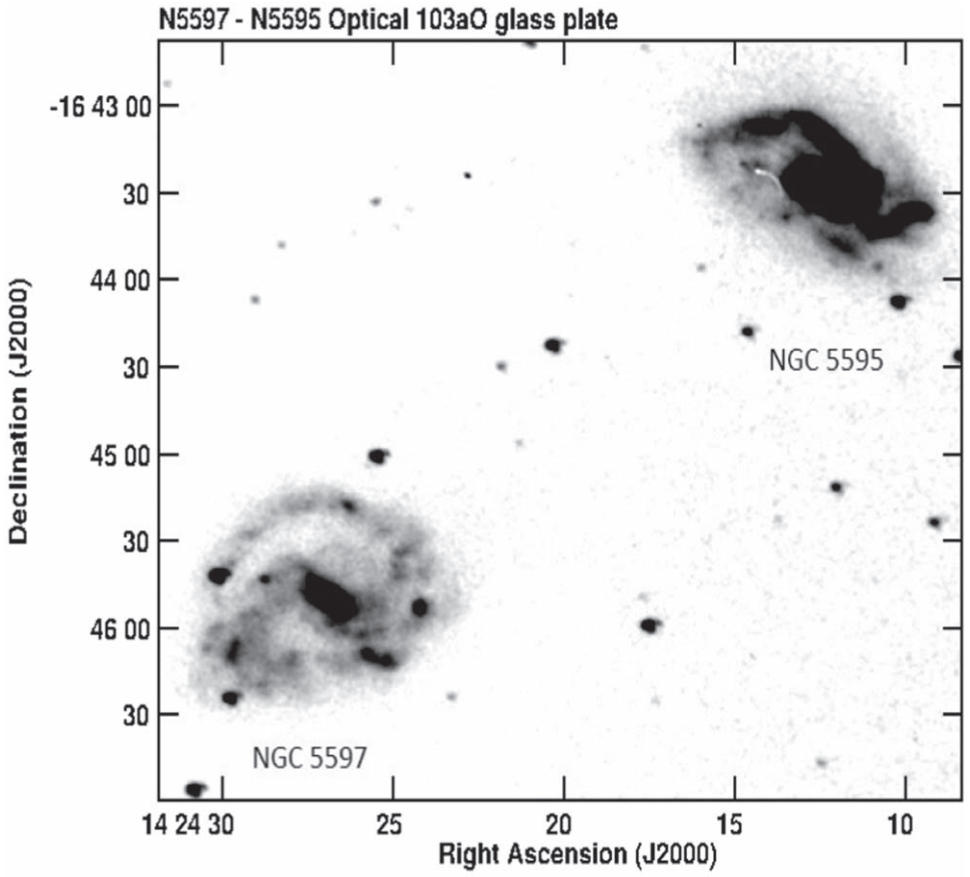

Figure 1. Reproduction of the optical blue continuum image (glass plate 103aO) from the close pair of disk galaxies NGC 5597 to the SE and NGC 5595 to the NW, obtained with the OAN-SPM 2.1 m optical telescope in Mexico (Diaz-Hernández et al. 2009). The flux density scale has not been calibrated. The gray scale is from $2 \rightarrow 27.8\sigma$, where σ is the noise in arbitrary units.

peak, seen in our VLA B-configuration spectrum of NGC 5597, is $\Delta V_{20\%} \sim 239.25$ km s^{-1}, while the full width at 50% of the peak is $\Delta V_{50\%} \sim 211.40$ km s^{-1} (see Figure 3, left panel). The Parkes and Green Bank single-dish radio telescopes did not have enough angular resolution to separate the two galaxies, resulting in spectra that showed the combined H I 21 cm emission from NGC 5595 and NGC 5597 (Mathewson et al. 1992; Springob et al. 2005). Figure 3 (middle) shows the rotation curve of NGC 5597 after several iterations with AIPS task GAL, assuming that the gas orbits are circular. This rotation curve was obtained in confocal circular annuli, each 8.″0 wide, integrated from $R = 0.''0$ to 70.″0 with both hemispheres (red- and blueshifted velocities compared to the systemic velocity; Rogstad et al. 1974). It shows a slowly rising curve with a low velocity value of $V \sim 24$ km s^{-1} at $R \sim 9.''23$ ($\sim$1.73 kpc) up to $V \sim 101$ km s^{-1} at $R \sim 61.''8$. The angular velocity curve, $\Omega_{\rm gas}$, shown in Figure 3 (right) decreases in such a way that it is less pronounced than a simple $\Omega_{\rm gas} \propto 1/(R^{3/2})$, perhaps suggesting an extended central mass distribution.[8]

4.1. NGC 5597 VLA B-configuration: Neutral Atomic Gas Spatial Distribution

At the angular resolution of our VLA observations (FWHM of $\sim 7.''1 \times 4.''2$), all of the H I 21 cm emission is from within the optical disk of NGC 5597.

[8] Modeling a detailed mass distribution in NGC 5597 is beyond the scope of the present study.

Figure 4 (left) shows the H I 21 cm VLA B-configuration integrated intensity over velocity (moment 0) superposed on itself in gray scale. Figure 4 (right) shows the optical *I*-filter image in contours superposed on H I (21 cm) moment 0 in gray scale. We note that all of the H I 21 cm cold gas emission arises from within the optical disk of the galaxy. Notice the narrow, curved, and long structures in H I in the NE with an abrupt decrease in emission toward the E side. The bright H I cold gas emission from the N lies at a mean distance of 5.8 ± 1 kpc, while the optical spiral arm (labeled 4 in Figure 2) lies at a mean distance of 6.9 ± 0.94 kpc on the plane of the sky. Also, there is a weak unresolved peak of H I emission, labeled A in Figure 4 (left), as if it were the center of a circular area of radius $\sim$15″ devoid of H I emission. At that spatial position, there is very weak (almost no) optical red emission (see Figure 2). As a comparison, other disk galaxies generally show H I 21 cm gas emission well beyond the optical disk, e.g., M83 (Rogstad et al. 1974); NGC 1300, SB(rs)bc (England 1989); NGC 3783, SBa (Garcia-Barreto et al. 1999); and NGC 3147, S(rs)bc (Haan et al. 2008).

Remarkably, in NGC 5597, there is no H I emission from the central region that includes the nucleus and circumnuclear area. Another area that lacks H I emission is located to the SW of the optical stellar bar and coincides with the odd SW optical spiral arm labeled 2 in Figure 2. It is worth noting that in other disk galaxies (e.g., M31), H I holes are associated with H II regions (Combes et al. 2002), with hot gas of $T \sim 10^4$ K (Spitzer 1978), or regions with newly formed stars.

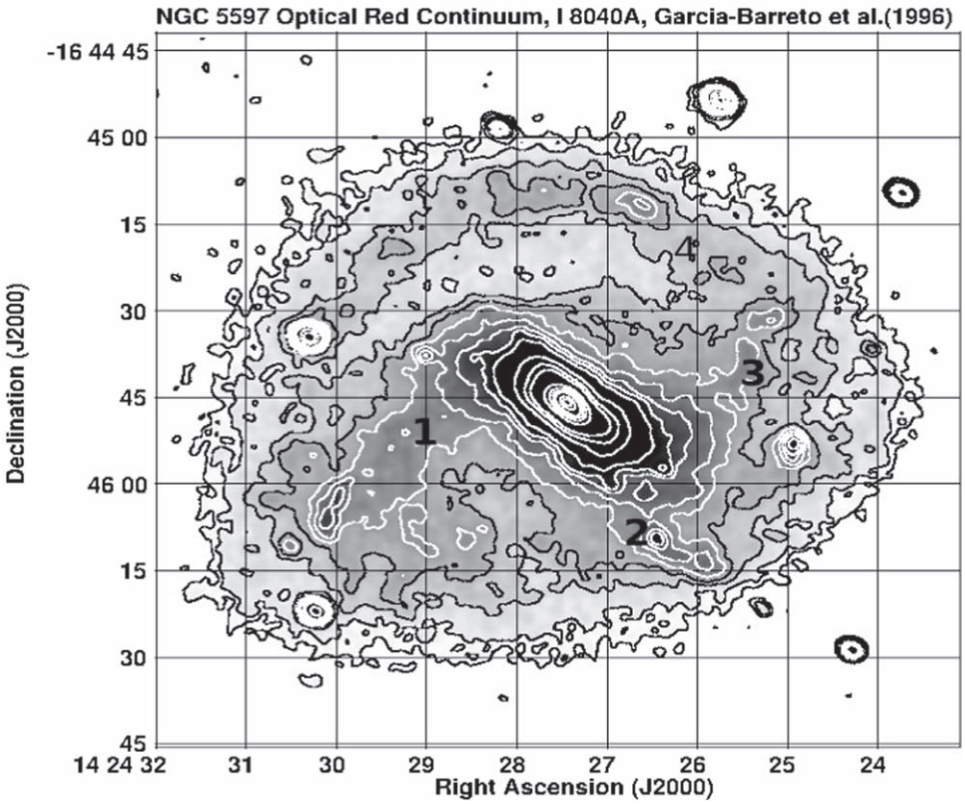

Figure 2. Reproduction of optical red continuum image (broadband filter *I* 8040 Å), in gray scale and contours, of the disk galaxy NGC 5597 obtained with the OAN-SPM 2.1 m optical telescope in Mexico (Garcia-Barreto et al. 1996). The image has been convolved with a circular Gaussian beam of $\sim 1\farcs5$ at FWHM. The flux density scale has not been calibrated; thus, the gray-scale stretch is from $5 \rightarrow 37\sigma$, where $1\sigma \sim 45$ is the noise in arbitrary units. Contours are at 5, 7, 11, 15, 20, 25, 30, 34, 40, 60, 80, 100, 200, 300, 400, 500, 750, 900 $\times$ 1σ.

Table 2
Spatial Positions of the Nucleus in NGC 5597 Measured in Various Bands/Images and the Positions of Other 20 cm Continuum Sources in NGC 5597

Image	α(J2000)	δ(J2000)	Source	Reference
		deg arcmin		
Name	hh mm ss	arcsec		
(1)	(2)	(3)	(4)	(5)
103aO	14 24 27.49	−16 45 45.9	Nucleus	1
I	14 24 27.44	−16 45 45.9	Nucleus	2
H I 21 cm	14 24 27.16	−16 45 46.64	Nucleus	3
Hα	14 24 27.34	−16 45 47.39	Peak of emission	2
20 cm cont.	14 24 27.40	−16 45 46.00	Nucleus[a]	3
20 cm cont.	14 24 28.03	−16 45 48.00	E on disk[b]	3
20 cm cont.	14 24 29.07	−16 45 40.00	NE on disk[c]	3
20 cm cont	14 24 29.91	−16 46 04.00	SE on disk[d]	3
20 cm cont.	14 24 27.47	−16 46 06.00	S on disk[e]	3
20 cm cont.	14 24 26.36	−16 45 49.00	W on disk[f]	3
20 cm cont.	14 24 24.97	−16 45 49.00	W on disk[g]	3
20 cm cont.	14 24 28.40	−16 45 07.00	N on disk[h]	3
Old 20 cm	14 24 27.45	−16 45 45.27	Nucleus	4
Old 20 cm	14 24 27.35	−16 45 45.27	Nucleus	4

Notes. The first old 20 cm radio continuum position by Condon et al. (1990) was with a circular beam FWHM $\sim 21\farcs0$. The second old position was with a circular beam FWHM $\sim 7\farcs0$.
(a) 53.9σ. (b) 6.7σ. (c) 4.2σ. (d) 3.8σ. (e) 4.2σ. (f) 4.3σ. (g) 4.1σ. (h) 3σ where $1\sigma \sim 167$ μJy beam^{-1}. These peaks of the 20 cm continuum sources are labeled a–h in Figure 7 (right panel).
References. (1) Diaz-Hernández et al. (2009); (2) Garcia-Barreto et al. (1996); (3) this work; (4) Condon et al. (1990).

Furthermore, there is no H I cold gas emission from the position of the optical nucleus, α(J2000) = $14^{\rm h}24^{\rm m}27\fs49$, δ(J2000) = $-16°45'45\farcs9$, or from the innermost circumnuclear region, where the gas is hot and ionized as indicated by the Hα continuum-free (Garcia-Barreto et al. 1996) and 20 cm radio continuum emission from that region (Condon et al. 1990) and our new VLA B-configuration 20 cm continuum image (see the following sections).

4.2. NGC 5597 VLA B-configuration: Neutral Atomic Gas Velocity Field and Kinematics

Our kinematical analysis of the H I 21 cm emission from NGC 5597 with the task GAL in AIPS is presented in Table 5.

Figure 5 shows the velocity field with small redshifted velocities (left) compared to the systemic velocity of NGC 5597 and with large redshifted velocities (right). The P.A. of the redshifted semimajor axis is $\sim$100° E of N, with the corresponding P.A. of zero velocities compared to systemic at $\sim$10° E of N.

Figure 6 (left) shows the velocity contour lines of the small blueshifted velocities, while Figure 6 (right) shows the large blueshifted velocity contour lines. To first order, the velocity field indicates a normal disk[9] in differential rotation, with the SW $\rightarrow$ S $\rightarrow$ SE $\rightarrow$ NE hemisphere showing redshifted

[9] In a normal disk galaxy in the approximation with only circular orbits ($v_R = 0$, $v_z = 0$), the velocity field will be symmetric about the minor axis, and one side will show redshifted velocities compared to the galaxy's systemic velocity, while the other side will show blueshifted velocities; see Figures 8–17 in Mihalas & Binney (1981) and Figure 3.6 in Combes et al. (2002).

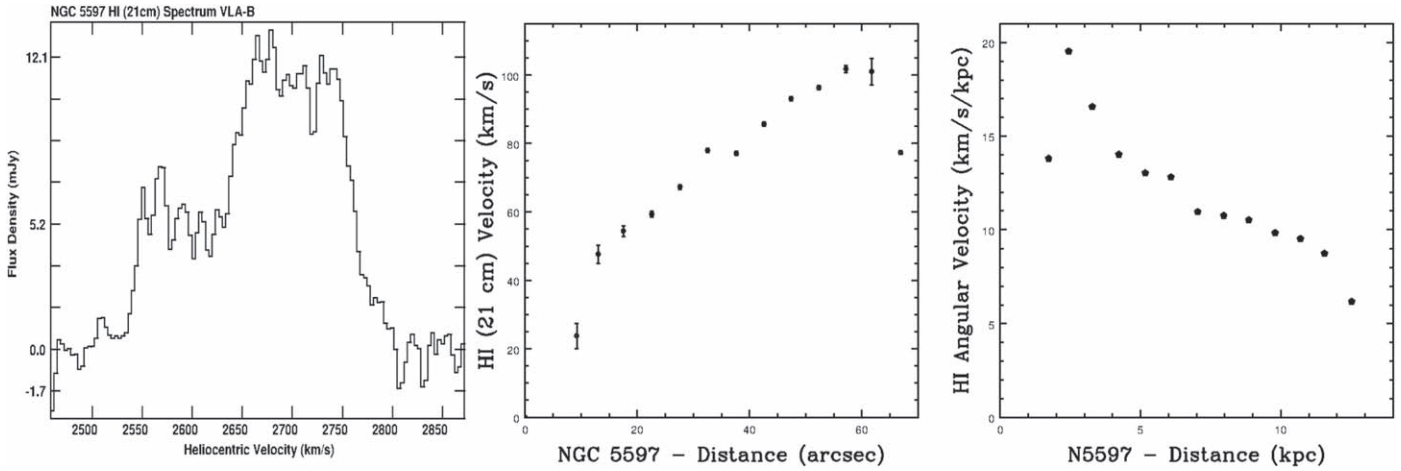

Figure 3. Left panel: H I 21 cm spectrum of NGC 5597 obtained from VLA B-configuration observations. The heliocentric systemic velocity, fitted by the task GAL in AIPS, is $V(\mathrm{sys})_{\mathrm{helio}} = 2698$ km s^{-1}, with $\Delta V_{50\%} \sim 211.40$ and $\Delta V_{20\%} \sim 239.25$ km s^{-1}. The flux density scale is very difficult to compare to previous Parkes (64 m) and Green Bank (91 m) single-dish spectra because their beam included both disk galaxies NGC 5595 and NGC 5597 (Mathewson et al. 1992; Springob et al. 2005). The shape of the spectrum looks very similar to that obtained with Nançay; however, its beam at FWHM was $\sim 3\farcm6$ E–W $\times$ 22′ N–S (Paturel et al. 2003). Middle panel: H I 21 cm rotation curve of NGC 5597. Right panel: H I 21 cm angular velocity curve of NGC 5597.

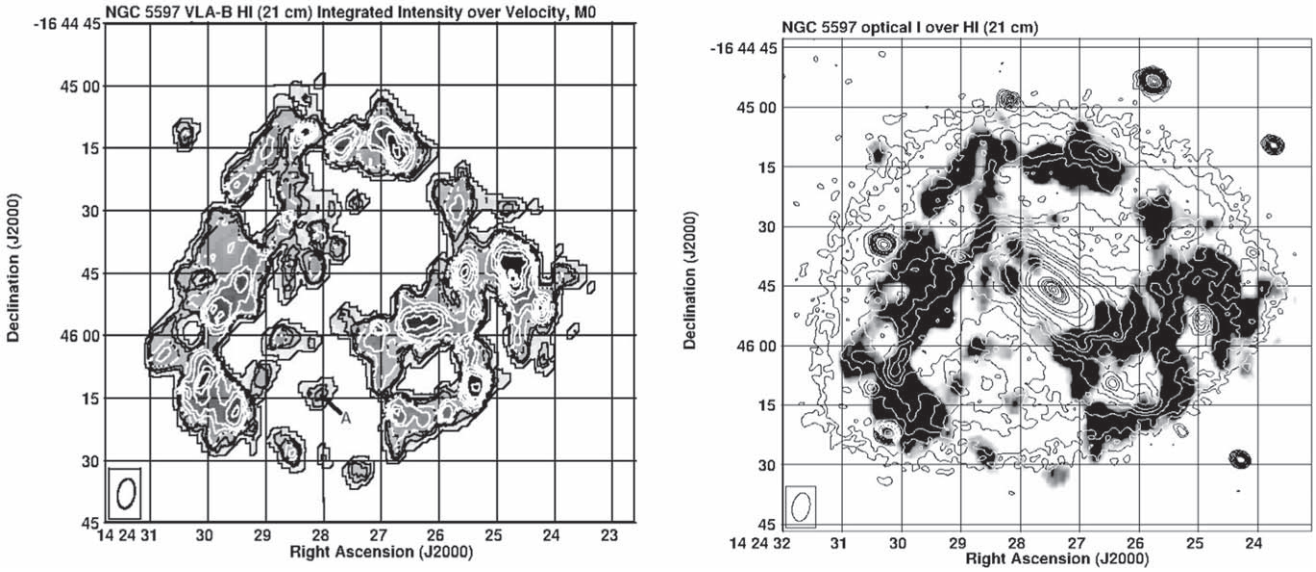

Figure 4. Left: H I 21 cm VLA B-configuration integrated intensity over velocity, moment 0, image of NGC 5597 in contours superposed on gray scale. The contours are at 3, 35, 50, 70, 100, 125, 150, 175, 200, 250, 270 $\times 1\sigma \sim 0.3$ mJy beam^{-1} km s^{-1}. The gray-scale stretch is from 3σ to 200σ. The synthesized beam at FWHM is shown in the lower left corner. The letter A indicates an isolated source as if it were in the center of a circular area devoid of H I emission. Right: optical *I*-filter image in contours (same as Figure 2) over H I (21 cm) moment 0 in gray scale, with gray-scale stretch from 2 to 17.5 mJy beam^{-1} km s^{-1}.

velocities, while the NE → N → NW → W hemisphere shows blueshifted velocities.

Taking the P.A. ∼ 100° E of N of the semimajor axis with redshifted velocities in NGC 5597 and assuming that the optical spiral arms are trailing, the hemisphere from NW clockwise to SE is closer to the observer, with the direction of the axis of rotation projected on the plane of the sky pointing SW at P.A. ∼ 190° E of N. As can be seen in Figure 4 (right), at this angular resolution and sensitivity, the H I 21 cm neutral cold gas is confined to the disk.

4.3. NGC 5597 VLA B-configuration: Neutral Atomic Gas Mass

The total integrated H I flux is $\int S_{\mathrm{HI}} dv \sim 2.9$ Jy km s^{-1} using the task IRING in AIPS with concentric rings, each $8\farcs0$ wide, from $R = 0\farcs0$ to $70\farcs0$ (Rogstad et al. 1974). The total estimated H I 21 cm atomic hydrogen mass in NGC 5597 is M(H I) $\sim 1.02 \times 10^9\ M_\odot$.[10] The dynamical mass in NGC 5597 is $M_{\mathrm{dyn}} \sim 2.6 \times 10^{10}\ M_\odot$, as measured from the observed maximum velocity; see Figure 3 (middle panel).[11]

[10] The H I 21 cm total mass in NGC 5597, and later in NGC 5595, was estimated from the known formula $M(\mathrm{H\,I}) = 2.356 \times 10^5 D^2 \int S_\nu dV$, where D is in megaparsecs, S_ν is in janskys, and dV is in kilometers per second (Wright 1974).

[11] The dynamical mass is estimated from the known formula resulting from the centrifugal force in circular orbits and the gravitational force from a central massive object; thus, one has the expressions for radial forces: $F_C = mV^2/R$, $F_G = GMm/(R^2)$. The object (cloud of gas) is in equilibrium of forces; thus, when we equal F_G to F_C, one obtains the expression $M_{\mathrm{dyn}} = 233.1V^2R$, where V is in kilometers per second, R is in parsecs, and the mass is in solar masses.

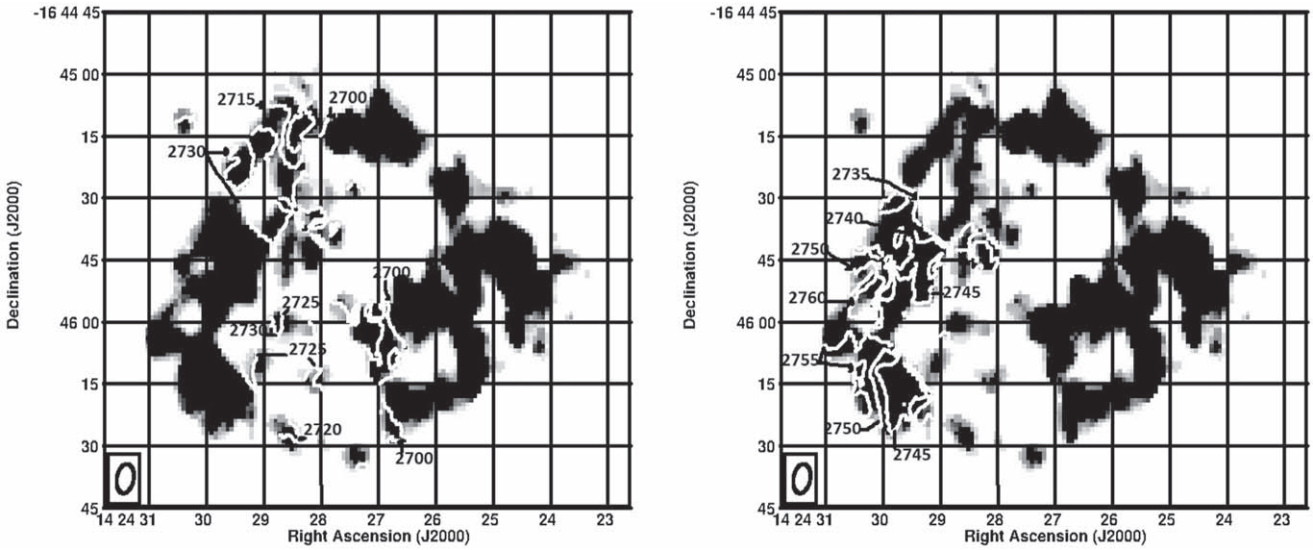

Figure 5. Redshifted H I 21 cm velocity field, moment 1, of NGC 5597 in contours superposed on the moment 0 gray-scale image. The gray scale in both panels ranges from 1 to 15 mJy beam^{-1} km s^{-1}. Left: low redshifted velocity contours from center to left at 2700, 2705, 2710, 2715, 2720, 2725, and 2730 km s^{-1}. Right: high redshifted velocity contours from center to left at 2735, 2740, 2745, 2750, 2755, and 2760 km s^{-1}.

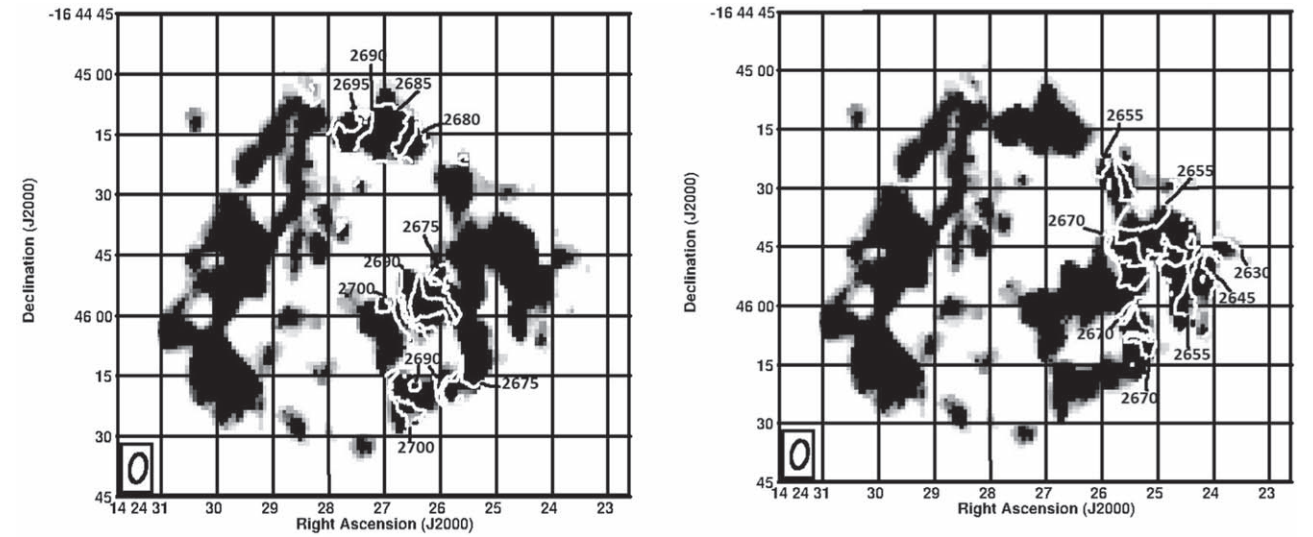

Figure 6. Blueshifted H I 21 cm velocity field, moment 1, of NGC 5597 in contours superposed on the moment 0 gray-scale image. The gray scale ranges from 1 to 15 mJy beam^{-1} km s^{-1}. Left: low blueshifted velocity contours from center to right at 2700, 2695, 2690, 2685, 2680, and 2675 km s^{-1}. Right: high blueshifted velocity contours from center to right at 2670, 2665, 2660, 2655, 2650, 2645, 2640, 2635, 2630, 2625, and 2620 km s^{-1}.

4.4. 20 cm Radio Continuum and Hα Emission from NGC 5597

Previous VLA 20 cm radio continuum emission observations of NGC 5597 by Condon et al. (1990) reported an unresolved central structure elongated at P.A. $\sim 43°$ E of N; see the last two values in Table 2.

We have produced a new 20 cm continuum emission image from our VLA B-configuration observing sessions, shown in Figure 7 (right), with a restoring beam at an FWHM of $\sim 6\farcs11 \times 3\farcs7$ (P.A. $\sim -8°$ E of N) and contours superposed on the optical red filter *I* image of NGC 5597 in gray scale (Garcia-Barreto et al. 1996). Our 20 cm radio continuum image, consistent with previously published images at a similar wavelength (Condon et al. 1990), shows a centrally peaked unresolved structure elongated along P.A. $\sim 15°$ E of N. The peak flux density of this structure is 9.02 mJy, and the rms noise in the image is $1\sigma \sim 167.4$ μJy beam^{-1}. Additionally, there are at least seven other weaker sources. They are all listed in Table 2 and shown in Figure 7 (right) with letters a–h.

The total flux density in our 20 cm image is 37 mJy. At the sensitivity of our observations, there is only one 20 cm radio continuum source with a peak flux density of 3σ in the optical N arm, labeled h, but it does not coincide with any weak Hα source (see Figure 7, left panel).

Figure 7 (left) shows a reproduction of our Hα+[N II] continuum-free image of NGC 5597 (Garcia-Barreto et al. 1996) in contours[12] superposed on the H I 21 cm moment 0 image in gray scale. The most intense Hα emission originates from an unresolved central source with its circumnuclear region and an elongated $13''$ structure at P.A. $\sim 32° \pm 14°$ E of N. Additionally, there are at least seven unresolved Hα sources

[12] The Hα+[N II] image was not flux density scale calibrated; thus, the contours are proportional to the rms noise in relative units.

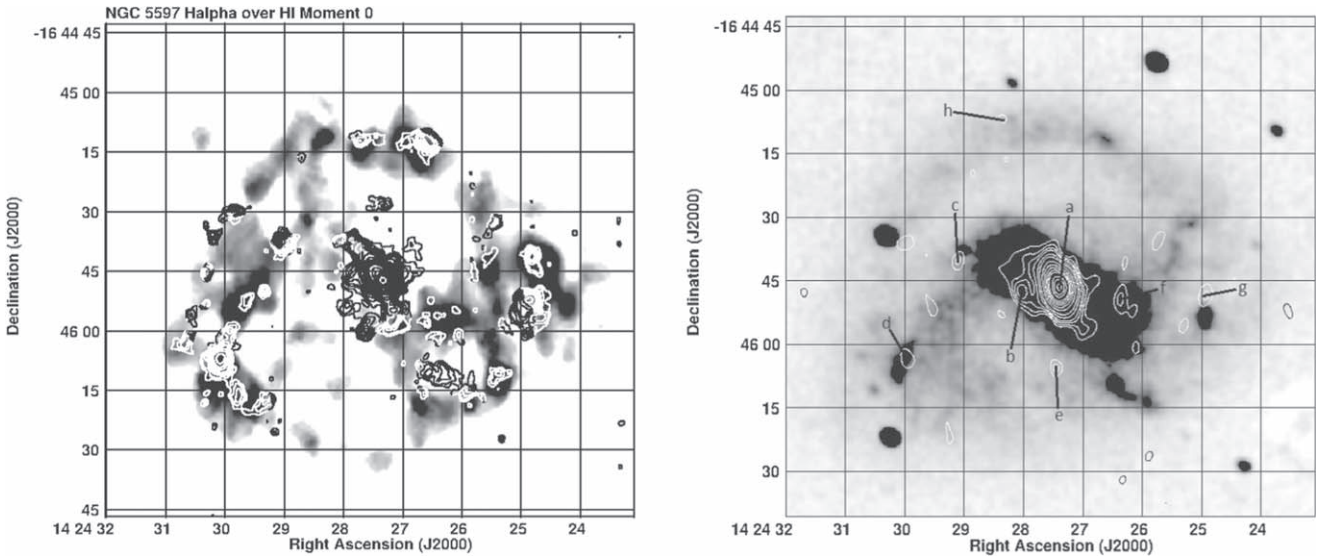

Figure 7. Left: reproduction of the Hα line emission image of NGC 5597 (Garcia-Barreto et al. 1996) in contours superposed on the H I 21 cm moment 0 in gray scale. The Hα image is not calibrated in flux density scale; therefore, the contours are proportional to the noise in arbitrary units from 3.5σ to 17σ. The most intense central emission of the hot gas, seen in Hα, is devoid of cold gas H I 21 cm emission. At least two Hα sources are offset by a few arcseconds to the N of the H I 21 cm sources. Right: our new 20 cm radio continuum emission image in contours superposed on the optical red (*I*-filter 8040 Å) image (Garcia-Barreto et al. 1996). The restoring beam size of the 20 cm continuum image at FWHM is $\sim 6\farcs11 \times 3\farcs7$ (P.A. $\sim -8°$). The contours are at 3σ, 4σ, 5σ, 6σ, 8σ, 10σ, 14σ, 18σ, 22σ, 26σ, 30σ, 40σ, 45σ, and 53σ, where $1\sigma \sim 167.4$ μJy beam^{-1}. The strongest 20 cm radio continuum emission arises from an unresolved source coincident with the position of the optical nucleus with an inner elongated structure at P.A. $\sim 25°$ E of N. The peaks of the 20 cm continuum sources are labeled a–h as listed in Table 2.

with low-intensity emission in their surroundings associated with the inner optical E arm structure (labeled 1 in Figure 2), at least two in the SW optical arm (labeled 2 in Figure 2), extended low-intensity emission associated with the optical arm (labeled 3 in Figure 2), and at least nine unresolved sources associated with the N arm (labeled 4 in Figure 2). The peak of the bright Hα emission from the N optical arm (labeled 4) is at a slightly larger distance than the peak of the H I 21 cm emission in that arm.

The lack of cold atomic H I 21 cm emission in the inner 20″, together with the presence of extended hot gas[13] in a P.A. similar to the P.A. of the rotation axis of the galaxy, may indicate the presence of a low-velocity bipolar outflow. While this extended hot gas might also be the result of central star formation, explaining its P.A. as seen in both Hα and 20 cm radio continuum would be a challenge.

All of the Hα sources throughout the disk indicate regions of massive O and B star formation with the ionization and recombination processes of atomic hydrogen (Spitzer 1978), with hot gas, $T \sim 10^4$ K, extending out of the plane of the galaxy. The temperature of the H I 21 cm gas presented in this paper, however, corresponds to an H I spin temperature of $T_s \leqslant 100$ K (Purcell & Field 1956; Field 1958; 1959; Wright 1974; Spitzer 1978; Combes et al. 2002). Assuming that the neutral gas distribution in NGC 5597 is similar to that in our galaxy, the H I 21 cm cold gas and sodium, Na I, are constituents of diffuse neutral clouds in a thin layer on the plane of the galaxy's disk (Spitzer 1978) with a thickness of probably less than 200 pc (Burton 1974).

[13] By hot gas, we mean gas from synchrotron plus thermal processes from observed Hα and 20 cm radio continuum optically thin emissions that indicate $T_e \sim 10^4$ K.

4.5. Central 20″ Gas Emission from NGC 5597

Figure 8 (right) shows the central innermost ∼20″ image of our new 20 cm continuum emission in contours obtained with the VLA in B-configuration. The image is superposed on the gray-scale image of the H I 21 cm moment 0 of NGC 5597. The peak of the 20 cm continuum emission at this angular resolution (FWHM of $\sim 6\farcs11 \times 3\farcs7$, P.A. $\sim -8°$) coincides fairly well with the position of the nucleus seen in the blue optical 103aO and red optical (*I* filter) images. Table 2 lists the positions of the center or nucleus[14] in NGC 5597, and they are also shown with different symbols in Figure 8.

The new 20 cm radio continuum map shows that the emission arises from an unresolved source with an elongated structure in the NE–SW direction at P.A. $\sim 17 \pm 7°$ E of N. This elongation is very comparable to the galaxy's rotation axis projected on the plane of the sky (direction P.A. $\sim 190°$ E of N or orientation P.A. $\sim 10°$ E of N). This NE–SW 20 cm radio continuum elongation is a true physical orientation and not due to a beam elongation artifact (since the beam P.A. $\sim -8°$ E of N). Also, it is in a similar orientation as the elongated structure seen in Hα, which we discuss further below.

The observed 20 cm continuum emission is a mixture of synchrotron process with high-velocity electrons interacting with an external magnetic field, $\boldsymbol{B}$,[15] and thermal process (free–free optically thin) with a typical electron temperature of $T_e \sim 10^4$ K from H II regions and/or supernova processes.[16]

Figure 8 (left) shows the Hα + [N II] continuum-free line emission contours superposed on the gray-scale VLA B-configuration H I 21 cm moment 0 map. Similar to the

[14] H I 21 cm kinematic, photometric 103aO, and *I* optical filters.

[15] For optically thin synchrotron emission, $S_\nu \propto B_\perp^{1.75} \nu^{-0.75} \theta^3$, while for the free–free emission for an optically thin case, $S_\nu \propto T_e^{-0.35} \nu^{-0.1} EM$.

[16] Future VLA radio continuum observations of NGC 5597 at a higher angular resolution and polarization analysis will be critical to better understanding the physical mechanisms and $\boldsymbol{E}$ (and $\boldsymbol{B}$) orientation.

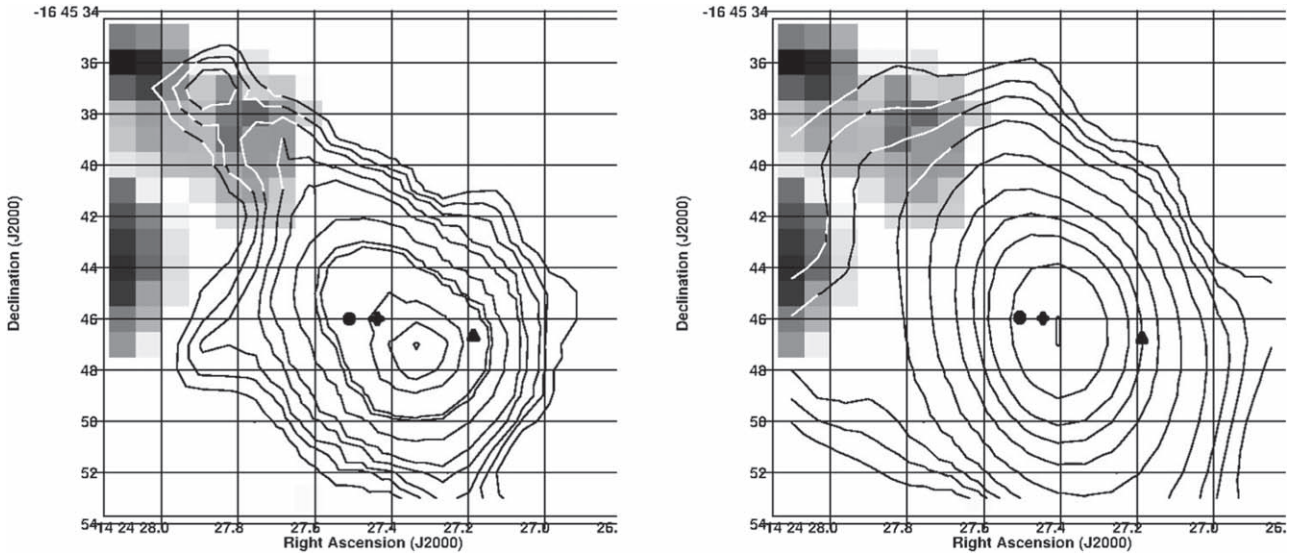

Figure 8. Innermost 20″ of NGC 5597. The filled triangle shows the kinematical center of the H I 21 cm emission, the four-pointed star shows the position of the photometric optical red *I*-filter image, and the filled circle shows the position of the photometric blue 103aO image. Spatial coordinates are listed in Table 2. Left: Hα continuum-free emission in contours superposed on the VLA B-configuration H I 21 cm moment 0 image in gray scale. The optical image is not calibrated in flux density scale, and the contour levels are at 7, 9, 11, 15, 20, 40, 80, 100, 300, 500, and 720 $\times$ 1σ, where 1σ = 10 in relative units. The gray scale ranges from 5.76 to 30 mJy beam^{-1} km s^{-1}. The extended emission lies at P.A. $\sim$ 32° $\pm$ 14°. Right: our new VLA B-configuration 20 cm continuum emission in contours superposed on the H I 21 cm moment 0 image in gray scale. The contour levels are the same as in Figure 8(b). The NE extended 20 cm radio continuum is at P.A. $\sim$ 17° $\pm$ 7°. The gray scale ranges from 5 to 25 mJy beam^{-1} km s^{-1}. Notice that the peak of the Hα emission (left panel) is slightly SW of the peak of the 20 cm radio continuum (right panel) that is associated with the optical nucleus. Qualitatively, both the 20 cm continuum and the Hα spatial emissions are similar. There is no cold gas atomic H I 21 cm emission (in gray scale) from the nucleus and the innermost circumnuclear region.

20 cm radio continuum emission, the Hα emission in the center of the galaxy originates from an unresolved source with an elongated structure in the NE–SW direction at P.A. $\sim$ 32° $\pm$ 14° or 212° $\pm$ 14°. This Hα emission comes from a recombination line process in the innermost H II circumnuclear region.

Both the central Hα and 20 cm radio continuum emissions are elongated in the NE–SW direction, and, qualitatively, their spatial extension is similar. The stellar bar (in the optical red, *I*, filter) lies at P.A. $\sim$ 52° and rotates at $\Omega_{\rm bar} \sim 15.3$ km s^{-1} kpc^{-1} (Garcia-Barreto et al. 1996; Garcia-Barreto & Momjian 2022). In that central region, there is no H I 21 cm emission. Furthermore, the spatial distribution of both the hot gas, seen in Hα, and the thermal/synchrotron 20 cm radio continuum suggests a bipolar geyser[17] into the innermost NE–SW direction with additional emission from an innermost circumnuclear region.

In both images in Figure 8, the H I 21 cm emission, shown in gray scale, is only seen from the extreme NE of the central 20″ region of NGC 5597. The peak of the Hα emission lies slightly SW of the optical photometric position of the nucleus (see Table 2). Although the small difference in these two positions might be due to astrometry, it might well be the correct spatial position of the SW Hα emission (brightest) from a bipolar nuclear geyser, as clearly observed in the barred disk galaxy NGC 1415, where there is weak or no Hα emission from the optical nucleus but two bright unresolved Hα sources from the lobes of a geyser (Garcia-Barreto et al. 1996, 2019; Garcia-Barreto & Moreno 2000). In this scenario, the NE lobe of such an Hα bipolar geyser or outflow in NGC 5597 might also exist; however, our image does not have the proper angular resolution to reveal it, especially that the emission is mixed with the elongated structure in the NE–SW direction (see Figure 7, left).

If the Hα and 20 cm radio continuum emission from NGC 5597 do indeed indicate a bipolar geyser or nuclear outflow, the hot ionized gas and relativistic electrons would be out of the plane of rotation of this galaxy, similar to, e.g., the large lobes seen in radio continuum in the barred galaxy NGC 3367 (Garcia-Barreto et al. 1998, 2002).

Although we are not yet aware of any published work on molecular gas emission in NGC 5597, one may expect a total $M(\rm H_2) \sim 6.4 \times 10^9$ $M_\odot$ from the CO–far-IR correlation (Scoville 1988). For example, molecular gas emission has been observed from the innermost central regions of two nearby bright barred galaxies like NGC 1068 (Planesas et al. 1991), where there is nuclear bipolar radio continuum emission (van der Hulst et al. 1982; Wilson & Ulvestad 1987), and NGC 3367 (Garcia-Barreto et al. 1998, 2002, 2005).

From the literature, there are many normal disk or barred galaxies with weak active galactic nuclei, such as the following four examples. (1) The normal disk galaxy M51, SA(s)bc pec has central mild activity that indicates the presence of a bidirectional jet, shown by an Hα + N[II] monochromatic image, optical red spectra, and radio continuum emission associated with the central region emanating from the nucleus, as seen in high angular resolution VLA observations (Ford et al. 1985; Cecil 1988; Crane & van der Hulst 1992; Ho & Ulvestad 2001). Furthermore, there is dense molecular gas in the inner $\leqslant$50 pc of M51 located in two blobs at P.A. $\sim$ 75°, perpendicular to the elongation of the optical Hα, and radio continuum images (Scoville et al. 1998). (2) Object NGC 1068, Sb(rs) II (Sandage & Tammann 1981) has a stellar bar (Scoville 1988), central molecular gas (Planesas et al. 1991), and a bipolar radio continuum nuclear source (Wilson & Ulvestad 1987). (3) Object NGC 1415, SBa

[17] The term "geyser" is utilized as a synonym of low-velocity (hundreds of kilometers per second) extragalactic nuclear outflow (Moody et al. 1995). In contrast, extragalactic plasma outflows, like in M87, have much higher velocities (many thousands of kilometers per second; Reid et al. 1989).

(Sandage & Tammann 1981) has two bright Hα unresolved sources straddling the nucleus, labeled A to the SE and B to the NW (Garcia-Barreto et al. 2019), which may be the result of a bipolar geyser with $v_{\rm rmgayser} \sim 140$ km s^{-1}. (4) Object NGC 3367, SBc(s) II (Sandage & Tammann 1981) has central molecular gas (Garcia-Barreto et al. 2005), central Hα emission (Garcia-Barreto et al. 1996), and a bipolar radio continuum source (Garcia-Barreto et al. 1998, 2002).

If one takes the velocity dispersion of stars in the innermost central region of each galaxy from the published literature (Ho et al. 2009) and uses the $M_{\rm BH}$–σ_* correlation relation (Gebhardt et al. 2000; Merritt & Ferrarese 2001a, 2001b), the mass of the supermassive black hole (SMBH) in each of these three barred galaxies is $M_{\rm NGC1068-BH} \sim 9.7 \times 10^7$, $M_{\rm M51-BH} \sim 7.6 \times 10^6$, and $M_{\rm NGC\ 3367-BH} \sim 1.4 \times 10^6\ M_\odot$. Thus, the observed central Hα emission, 20 cm radio continuum emission, and central H I 21 cm hole in all of these barred galaxies may indeed be the result of a central SMBH.

As a comparison, the masses of the SMBHs in two normal disk galaxies observed with nuclear geysers or bipolar outflows, namely, M81 (NGC 3031; Sb(r)I-II) and M101 (NGC 5457, Sc(s) I), using the same $M_{\rm BH}-\sigma_*$ correlation are $M_{\rm M81-BH} \sim 5.4 \times 10^7$ and $M_{\rm M101-BH} \sim 3.97 \times 10^4\ M_\odot$, respectively (Garcia-Barreto et al. 2019).

In the case of the barred galaxy NGC 5597, one of the two galaxies in this study, the central observed distribution of the Hα emission, 20 cm radio continuum emission, and H I 21 cm hole all seem to suggest the existence of an SMBH with $M_{\rm NGC\ 5597-BH} \sim 10^6\ M_\odot$.

5. NGC 5595: A Late-type Disk Galaxy

5.1. General Characteristics

Galaxy NGC 5595 is classified as Sc(s)II (Sandage & Tammann 1981), SAB(rs)c (de Vaucouleurs et al. 1993). It is a member of a close pair with NGC 5597 to the SE at a projected angular distance on the plane of the sky of ∼3.″97 (Garcia-Barreto et al. 2003). As mentioned earlier in the case of NGC 5597, they both have very similar systemic velocities and are close on the plane of the sky; therefore, we also adopt its distance as $D_{\rm pair} = 38.6$ Mpc (Tully 1988; $1'' \sim 187.14$ pc). Figure 1 shows its blue continuum optical emission from our 103aO observation (Diaz-Hernández et al. 2009). As in the case of NGC 5597, astrometry was done to independently estimate its photometric position (Diaz-Hernández et al. 2009). See Table 4 for its basic properties.

5.2. VLA B-configuration H I 21 cm Observations

As previously discussed in the section on NGC 5597, the Parkes and Green Bank single-dish radio telescopes did not have enough angular resolution to separate the two galaxies, resulting in spectra that showed the combined H I 21 cm emission from both NGC 5595 and NGC 5597 (Mathewson et al. 1992; Springob et al. 2005). Only the Nançay radio telescope, with an FWHM beam size of ∼3.′6 E–W × 22′ N–S, was able to isolate the H I 21 cm emission spectrum of NGC 5595 with a peak flux density of ∼100 mJy and a velocity range of ∼2525–2875 km s^{-1} (Paturel et al. 2003).

Figure 9 (left) shows our VLA B-configuration H I 21 cm spectrum from NGC 5595 using the task *ISPEC* in AIPS. The shape is very similar to the Nançay spectrum (Paturel et al. 2003). Using the AIPS task GAL, the fitted kinematic H I 21 cm systemic velocity is $V_{\rm sys} \sim 2702$ km s^{-1} using both redshifted and blueshifted velocities. The measured velocity widths in the spectrum obtained from our VLA B-configuration observations are $\Delta V_{50\%} \sim 317.5$ and $\Delta V_{20\%} \sim 345$ km s^{-1} at 50% and 20%, respectively. Figure 9 (middle) shows the rotation curve from NGC 5595 from our fit assuming circular orbits (Rogstad et al. 1974). It has a high value from a small radius, decreases a little bit, and then continues slowly rising all the way to 90″. Finally, Figure 9 (right) shows the NGC 5595 angular velocity ($\Omega_{\rm gas} \equiv V(R)/R$); notice its very smooth decreasing values.

5.3. H I 21 cm Spatial Distribution and Kinematics

Figure 10 shows the VLA B-configuration H I 21 cm velocity-integrated moment 0 map from NGC 5595 in contours superposed on itself in gray scale. Most of the emission originates from giant H I 21 cm clouds in normal differential rotation around the nucleus of the disk galaxy. The spatial extent of the H I 21 cm emission spans ΔR.A. ∼ 18$^{\rm s}$–09$^{\rm s}$ and Δdecl. ∼ −16°42′15″ to −16°44′10″. Notice that the optical N spiral arm in NGC 5595 is assumed to be trailing (e.g., Figure 1). However, the NE H I 21 cm extended morphology on the plane of the sky appears as if it were a leading structure.[18]

We also note the lack of H I 21 cm emission from the central region, where there seems to be a circumnuclear radio continuum structure (see Section 5.5).

Figure 11 shows our VLA B-configuration H I 21 cm velocity field. The kinematical parameters are listed in Table 3. The left panel shows the contours of the blueshifted velocities (compared to systemic velocity), while the right panel shows the contours of the redshifted velocities from the center to the SW. The NE → N → SW hemisphere is closer to the observer, and the projection on the plane of the sky for the orientation of the rotation axis of the disk galaxy is at P.A. ∼ 327 E of N, with a direction pointing to the NW.

Figure 10 (as well as Figures 11 and 12) reveals for the first time the existence of extended H I 21 cm cold gas structures to the NE and SW of disk galaxy NGC 5595 with no blue optical continuum or 20 cm radio continuum counterparts. The approximate lengths of the H I 21 cm tails to the NE and SW of NGC 5595 on the plane of the sky are ∼7 and ∼4.2 kpc, respectively. The NE contours show blueshifted velocities as if they were a smooth continuation of the blueshifted velocities from the inner disk. Similarly, the lowermost SW contours show redshifted velocities as if they were a smooth continuation of the redshifted velocities from the inner disk. Both (NE and SW) extended structures seem to be warps of the NGC 5595 disk.[19]

Figure 12 shows the reproduction of the blue optical continuum 103aO emission from NGC 5595 in contours (Diaz-Hernández et al. 2009) superposed on the H I 21 cm moment 0 map in gray scale (see Figure 10). The blue optical image is not flux calibrated, so the contours are proportional to a 1σ noise level in arbitrary units.

As mentioned earlier, the NE H I 21 cm extension morphology is peculiar, since it shows blueshifted velocities and appears, on the plane of the sky, as if it were a leading

[18] This could be a plausible result of a flat retrograde parabolic passage of a companion of equal mass; see Figure 1, $t = 4$, in Toomre & Toomre (1972).
[19] The large-scale warps of disk galaxies remain a challenge for theorists (Toomre 1983).

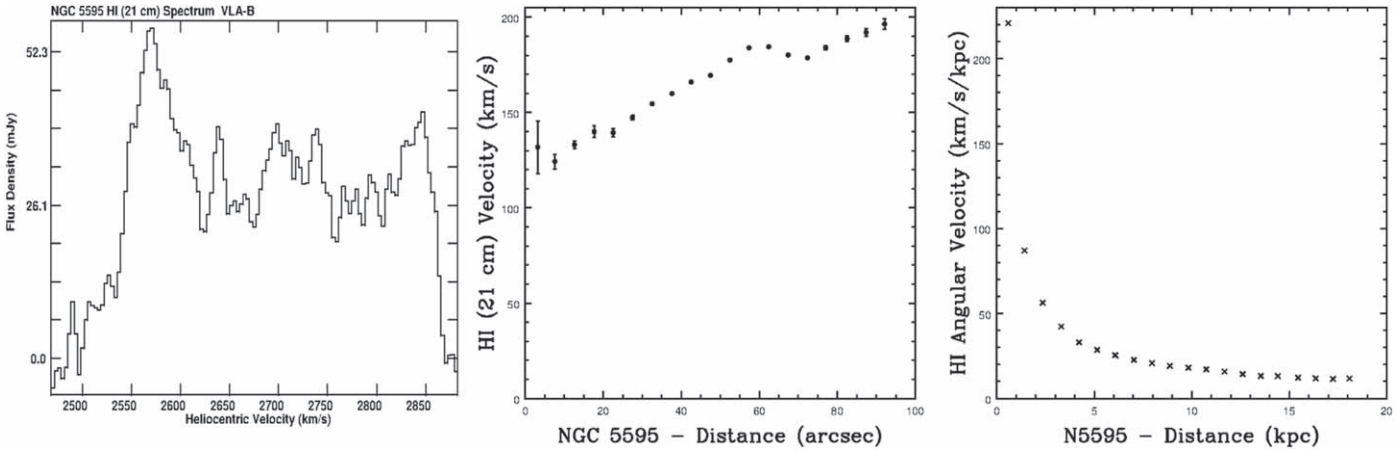

Figure 9. Left: H I 21 cm spectrum obtained from our VLA B-configuration observations of the disk galaxy NGC 5595. The heliocentric systemic velocity, fitted by the task GAL in AIPS, is $V(\mathrm{sys})_{\mathrm{helio}} = 2702$ km s^{-1}, with $\Delta V_{50\%} \sim 317.5$ and $\Delta V_{20\%} \sim 345$ km s^{-1}. The flux density scale of the spectrum is very difficult to compare to previous ones obtained with the Parkes (64 m) and Green Bank (91 m) radio telescopes because their beams included both disk galaxies, NGC 5595 and NGC 5597 (Mathewson et al. 1992; Springob et al. 2005). The shape of the spectrum looks very similar to that obtained with Nançay; however, its beam at FWHM was $\sim 3\farcs6$ E–W $\times$ 22′ N–S (Paturel et al. 2003). Middle: NGC 5595 H I 21 cm rotation curve. Right: NGC 5595 H I 21 cm angular velocity Ω_{gas}.

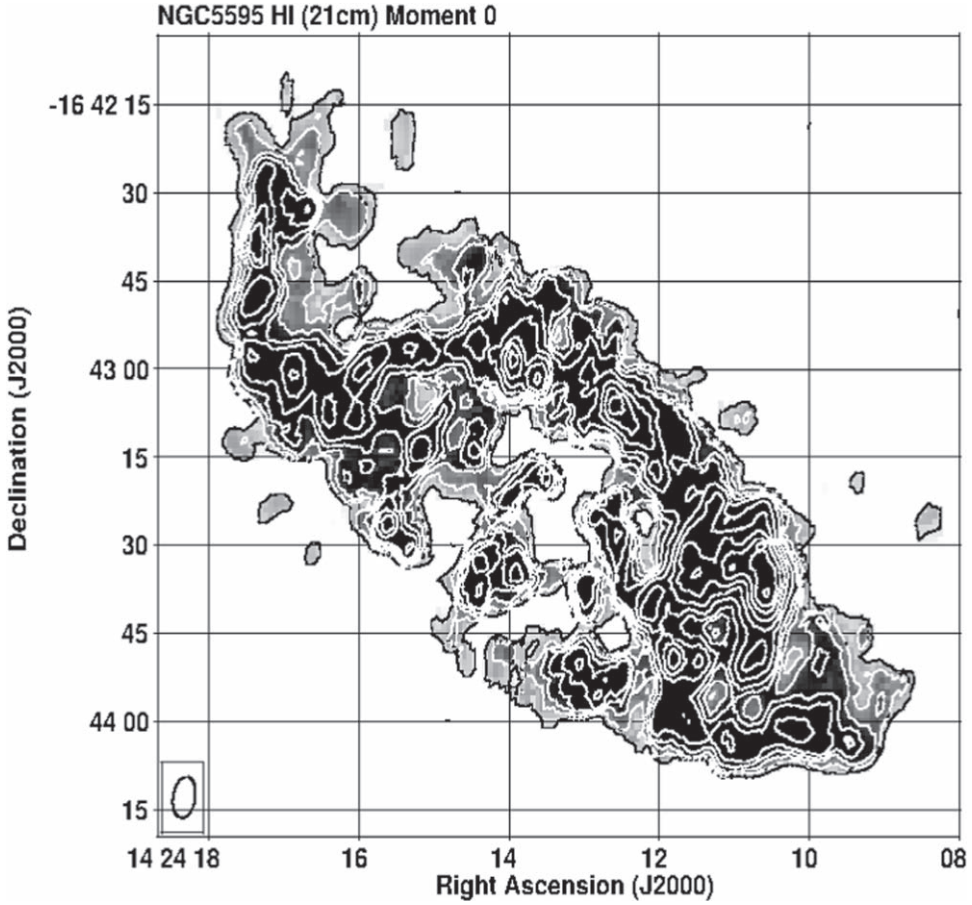

Figure 10. The NGC 5595 VLA B-configuration H I 21 cm integrated intensity over velocity, moment 0, image in gray scale and contours. The contour levels are at 3, 6, 9, 12, 15, 20, 25, 30, 35, 40, and 47 $\times$ 1σ = 3.3 Jy beam^{-1} km s^{-1}. Notice that there is no atomic hydrogen gas emission from the position of the kinematical center α(J2000.0) = $14^{\mathrm{h}}24^{\mathrm{m}}13\overset{\mathrm{s}}{.}3$, δ(J2000.0) = $-16°43'21\farcs6$. This position coincides with the optical continuum photometric center. The VLA B-configuration beam size, which is $\sim 7\farcs14 \times 4\farcs21$ at FWHM, is shown in the lower left corner.

structure; the N optical (blue) spiral arm is assumed to be trailing and also shows blueshifted velocities. The NE and SW H I 21 cm elongated emissions may be filamentary gas structures that are most likely a result of a recent gravitational tidal interaction with its neighbor, NGC 5597. Similar extended structures have been observed in the M82 galaxy (Yun et al. 1993) and shown to exist from computer simulations (Toomre & Toomre 1972; Mihos & Hernquist 1996).

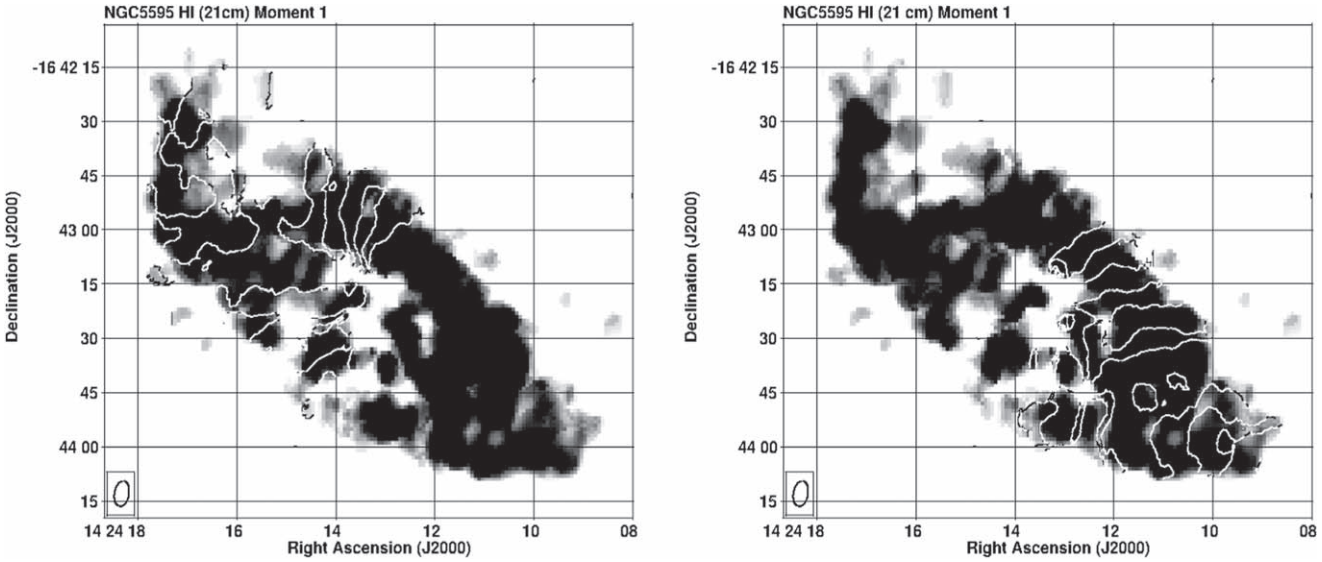

Figure 11. The left panel shows the H I 21 cm velocity field of NGC 5595, moment 1, with blueshifted velocities in contours superposed on the moment 0 image in gray scale (the scale stretch is from 7.7 to 37 mJy beam^{-1} km s^{-1}). Velocity contours from center to NE are at 2690, 2670, 2650, 2630, 2610, 2590, 2570, 2560, and 2550 km s^{-1}. The right panel shows the redshifted velocity contours from center to SW at 2700, 2720, 2740, 2760, 2780, 2800, 2820, 2840, 2850, and 2855 km s^{-1}. The velocity field indicates differential rotation, as expected from a disk galaxy. Notice that the uppermost NE contours show blueshifted velocities as if they were a smooth continuation from the blueshifted velocities from the inner disk, although the cold atomic H I 21 cm gas there has no optical counterpart. Similarly, the SW contours show redshifted velocities as if they were a smooth continuation from the redshifted velocities from the inner disk, although the cold atomic H I 21 cm gas there has no optical counterpart.

Table 3
Kinematical H I 21 cm VLA B-configuration Analysis of the Disk Galaxy Pair NGC 5595 and NGC 5597

Galaxy Name (1)	α(J2000) (hh mm ss) (2)	δ(J2000) (deg arcmin arcsec) (3)	P.A.[a] (deg E of N) (4)	Inclination (deg) (5)	V(H I)$_{\rm helio}$ (km s^{-1}) (6)
NGC 5595	14 24 13.31	−16 43 21.59	237	56	2702
NGC 5597	14 24 27.16	−16 45 46.64	100	36	2698

Note.
[a] P.A. of the semimajor axis of redshifted velocities.

5.4. NGC 5595: Cold Hydrogen Atomic Gas Mass

The total H I 21 cm gas mass in NGC 5595 is M(H I) $\sim 2.9 \times 10^9$ $M_\odot$. The dynamical mass in NGC 5595 is $M_{\rm dyn} \sim 1.3 \times 10^{11}$ $M_\odot$ as measured from the observed maximum velocity; see Figure 9 (middle panel).

5.5. NGC 5595: Our VLA B-configuration 20 cm Radio Continuum Emission Map

Previously published 20 cm VLA radio continuum observations with an angular resolution of $\sim$21″ at FWHM showed an unresolved central source in NGC 5595 elongated into the NE–SW orientation (Condon et al. 1990), while at an angular resolution of $\sim$7″ at FWHM, the VLA image also showed an unresolved central source with at least three other weaker peaks of emission and weak extended emission surrounding them. All of the 20 cm radio continuum emission reported arises from the disk of NGC 5595 (Condon et al. 1990).

We have produced a new 20 cm radio continuum emission image from our VLA B-configuration observations with an angular resolution of $\sim$6.″11 × 3.″7 at FWHM (P.A. $\sim -8°$ E of N). This continuum image is shown in Figure 13 in contours superposed on the reproduction of the blue optical continuum 103aO image in gray scale. The 20 cm continuum image shows an unresolved dominant central source with a peak flux density of 2.59 mJy at $\alpha \sim 14^{\rm h}24^{\rm m}13\overset{\rm s}{.}203$, $\delta \sim -16°\ 43'\ 21.''99$. This position coincides with the photometric blue optical continuum 103aO nucleus and the kinematic H I 21 cm center (see Tables 1 and 4). Additionally, there are other 20 cm continuum sources in what seems to be a circumnuclear region within an angular distance from the nucleus of $R_{\rm N-CNR} \sim 9.''5$ or a linear distance of $R_{\rm N-CNR} \sim 1.77$ kpc. There are also 20 cm continuum sources associated with the N and SW spiral arms within the disk. The total 20 cm radio continuum flux density in our new image obtained with the VLA in B-configuration is $\sim$81.83 mJy.

Our new VLA B-configuration 20 cm radio continuum image shows that, at the sensitivity of the observations, all of the 20 cm radio continuum emission originates from the optical disk of NGC 5595 (see Figure 13). At the position of the unresolved dominant central 20 cm radio continuum emission, there is no H I 21 cm neutral cold gas emission (see Figures 10). The origin of the 20 cm radio continuum emission is most likely a mixture of thermal ($T_e \sim 10^4$ K) and optically thin synchrotron processes related to star formation (H II regions) and their evolution (supernovae). There is no 20 cm radio continuum emission from the uppermost NE and lowermost SW structures that exhibit H I 21 cm emission as seen in the moment 0 image (see Figures 10–12).

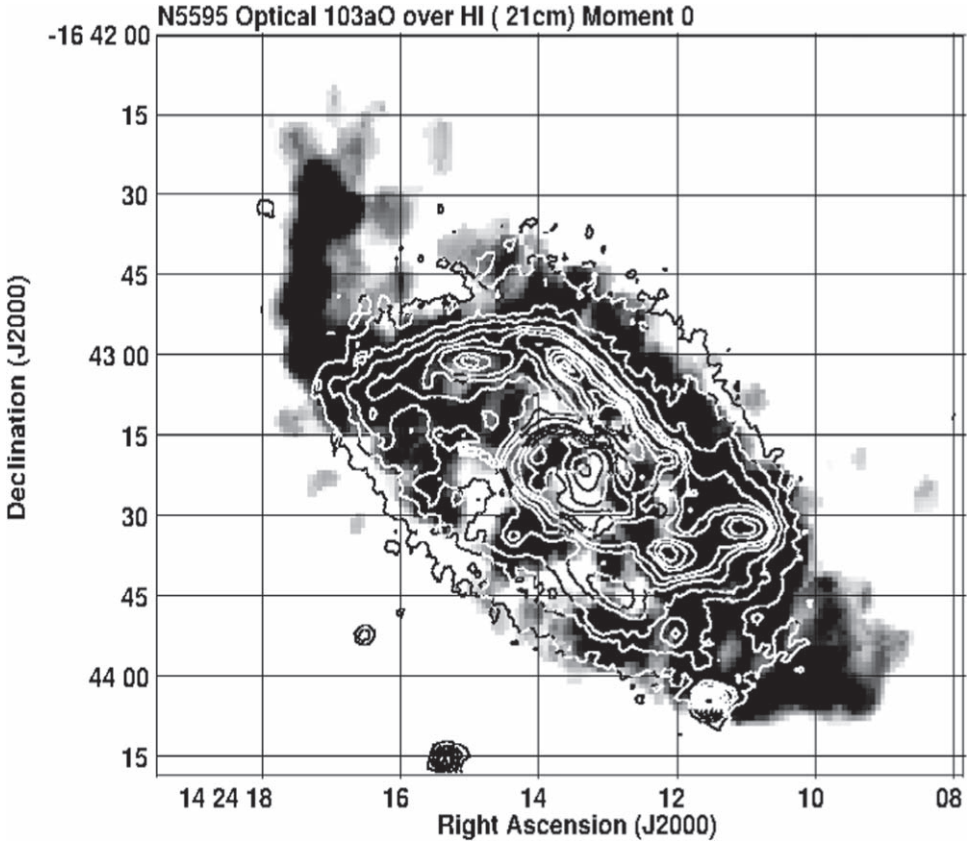

Figure 12. Reproduction of the 103aO blue optical emission of NGC 5595 (Diaz-Hernández et al. 2009) in contours superposed on the H I 21 cm moment 0 image in gray scale. Optical emission is not flux calibrated; its contours are at 4.7, 9, 13, 20, 25, 30, 40, 46, 53, 60, 75, and 92 $\times$ 1σ, where 1$\sigma \sim$ 90 in arbitrary units proportional to intensity. The gray-scale stretch is from 6.6 to 37 mJy beam^{-1} km s^{-1}. Notice that the H I 21 cm NE and SW elongated structures do not have optical continuum emission counterparts.

6. No Tidal Filamentary Structures between the Field of the Pair Disk System NGC 5595 and NGC 5597

The isolated galaxy pair NGC 5597–NGC 5595 is in an area of the universe with very low galaxy volume density (Tammann 1985; Tully & Fischer 1987); therefore, there is no hot intergalactic gas that could have stripped the atomic gas from the outer disk radii. Thus, it seems that both NGC 5595 and NGC 5597 originated with just enough H I atomic neutral gas to form their disks and stars.

The blue continuum image (Figure 1) does not show any extended optical emission or bridges between NGC 5595 and NGC 5597; this fact might indicate that this pair of galaxies is in the early stage of gravitational interaction (Toomre & Toomre 1972; Mihos & Hernquist 1996; Linde & Mihos 2022).

However, our VLA B-configuration observations of both disk galaxies with an angular resolution of $\sim$7.″14 $\times$ 4.″2 at P.A. $\sim -11^{\circ}$ E of N show that the H I 21 cm emission from NGC 5597 is confined to the extent of its optical disk, while in NGC 5595, the H I 21 cm emission is from its disk, as well as from structures to the NE and SW that do not have blue optical or 20 cm continuum counterparts (see Figures 1, 10, and 12).

Computer simulations of gas dynamics and starbursts in disk mergers of similar mass suggest that as the galaxies approach, they become severely distorted, forming long tidal tails and a bridge connecting the two disk galaxies (Barnes 1990; Mihos & Hernquist 1994, 1996; Barnes 1998). A recent retrograde passage dynamical model of M101 and NGC 5474 reproduces the observations well while suppressing the formation of long tidal tails (Linde & Mihos 2022). The spatial distribution of the cold atomic H I 21 cm gas, especially toward the NE and SW, outside the optical disk in NGC 5595 suggests that the pair system NGC 5595–NGC 5597 is in a very early phase of its gravitational interaction with perhaps a retrograde passage (Linde & Mihos 2022).

Table 4 lists the different intrinsic parameters of both galaxies, including the estimated dynamical masses. The angular separation of the galaxies on the plane of the sky is 3.″97, and the ratio of their dynamical masses is $M_{\rm dyn}^{\rm NGC5595}/M_{\rm dyn}^{\rm NGC5597} \sim 5$.

From the empirical observational studies of radio continuum emission from pairs of disk galaxies, the central sources in barred galaxies are more powerful than in nonbarred ones (Hummel et al. 1990). In our study, the barred galaxy NGC 5597 has a nuclear unresolved 20 cm radio continuum source that is about 3.5 times more powerful than the similar source in NGC 5595. Furthermore, the innermost central region of NGC 5597 shows Hα and 20 cm radio continuum emission elongated in the NE–SW orientation (at a P.A. not far from the P.A. of the rotation axis). This innermost region has no H I 21 cm atomic gas emission, while the galaxy shows an H I gas angular velocity curve $\Omega_{\rm gas}$ that is different than the expected $\Omega_{\rm gas} \propto R^{-1}$ for a spiral disk galaxy, suggesting an excess of mass. All of these observational facts suggest that gas has recently been supplied as fresh fuel into the barred galaxy NGC 5597, while there are H I 21 cm extended structures to the NE and SW in disk galaxy NGC 5595.

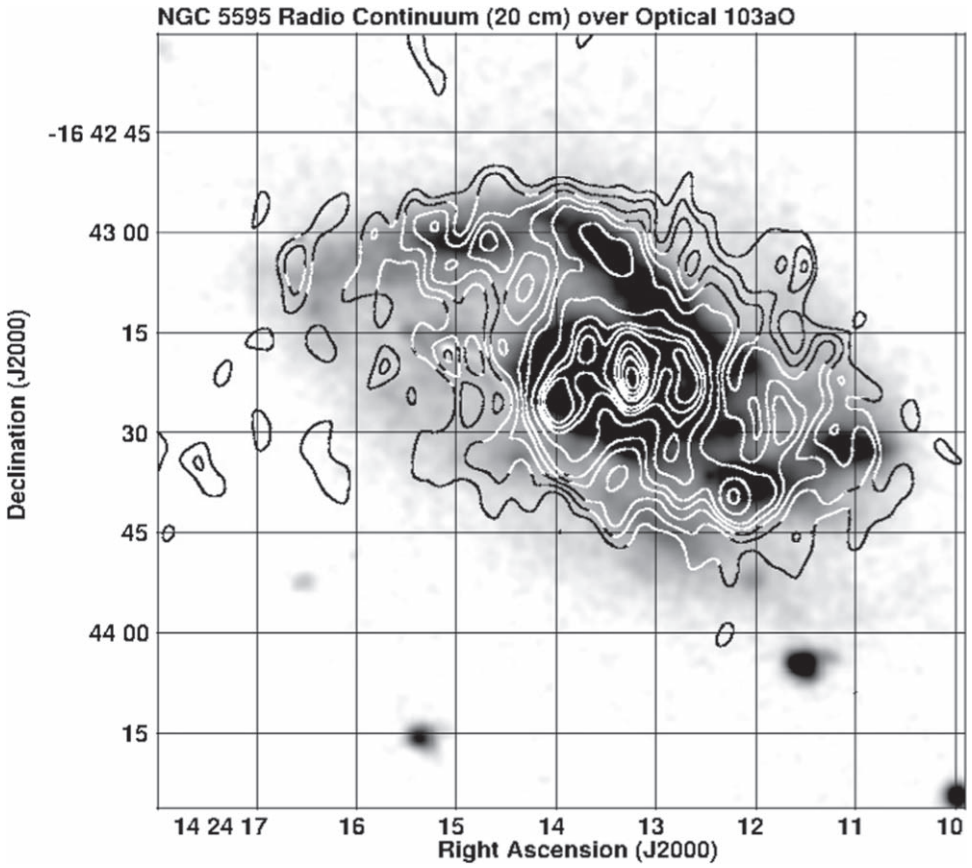

Figure 13. Our VLA B-configuration 20 cm radio continuum emission from disk galaxy NGC 5595 in contours superposed on the reproduction of the 103aO blue optical emission from NGC 5595 (Diaz-Hernández et al. 2009) in gray scale. Contours are at 3, 4, 5, 6, 8, 10, 11, 12, 14, 15, and 15.6 × 1σ, where 1$\sigma \sim 167$ μJy beam^{-1}. The brightest 20 cm radio continuum source coincides with the optical nucleus. Two other sources at a distance of $\sim$10″ from the center toward the E and W might be part of a circumnuclear structure. There is weak emission from almost all over the optical disk but no 20 cm radio continuum emission from either the NE or the SW H I 21 cm extended structures (see Figure 11).

Table 4
Properties of Disk Galaxy Pair NGC 5595 and NGC 5597

Data (1)	NGC 5595 (2)	NGC 5597 (3)
Optical diameter	$\sim$1.″6	$\sim$1.″87
m_v	12.6	13.1
V_{sys}	2702 km s^{-1}	2698 km s^{-1}
M_{HI}	2.9 × 10^9 $M_\odot$	1 × 10^9 $M_\odot$
M_{dyn}	1.3 × 10^{11} $M_\odot$	2.6 × 10^{10} $M_\odot$
L_{FIR}^{IRAS}	2.22 × 10^{10} $L_\odot$	2.21 × 10^{10} $L_\odot$
P.A.$^{red}_{semimajor-axis}$	237° E of N	100° E of N
P.A.$_{rotation-axis}$	327° E of N	190° E of N
Direction$_{rotation-axis}$	NW	SW
Peak flux density (20 cm)	2.593 mJy beam^{-1}	9.02 mJy beam^{-1}
Total flux density (20 cm)	81.83 mJy	36.99 mJy

We have made a low angular resolution moment 0 image to search for extended H I 21 cm emission from the field of the pair system NGC 5595 and NGC 5597 using our VLA B-configuration observations, restricting the *uv* range from zero to only 5 kλ (Figure 14). This resulted in a synthesized beam with an FWHM of $\sim$30.″7 × 28.″8 at P.A. $\sim$ +50° E of N and 1$\sigma \sim$ 19.45 mJy beam^{-1} km s^{-1}.

Figure 14 shows no extended intergalactic H I 21 cm emission from any filaments or bridges and only slightly extended emission from the S, SW, and W of NGC 5597 and NE, SE, and SW of NGC 5595.[20]

This negative observational result (no long tidal tails between NGC 5595 and NGC 5597) is interesting and important because NGC 5597 and NGC 5595 are very close not only on the plane of the sky but also physically, as they both have very similar recession velocities. Table 4 shows the general properties of both NGC 5595 and NGC 5597. These two galaxies also reside in a low galaxy density environment (Tammann 1985; Tully & Fischer 1987). The NGC 5597–NGC 5595 system must be in an early stage of gravitational interaction; if it were in an advanced stage, the NGC 5595–NGC 5597 pair system would resemble the Antennae or Mice galaxy pairs (Toomre & Toomre 1972; Barnes 1990; Mihos & Hernquist 1996; Barnes 1998; Linde & Mihos 2022). As a comparison, a long tidal H I 21 cm atomic neutral hydrogen gas structure has been detected in the M51–NGC 5195 system, which is within 5′ on the plane of the sky (Rots et al. 1990); extended filamentary H I 21 cm atomic neutral hydrogen gas structures have been detected from the M81–M82–NGC 3077 system, which is within 80′ on the plane of the sky

[20] The lack of extended intergalactic H I 21 cm emission from any filaments or bridges may be due to low surface brightness sensitivity. Future VLA H I 21 cm observations with lower angular resolution and deeper integrating, and therefore better surface brightness sensitivity, will clarify the existence of any intergalactic neutral atomic hydrogen gas in the disk galaxy pair NGC 5595 and NGC 5597.

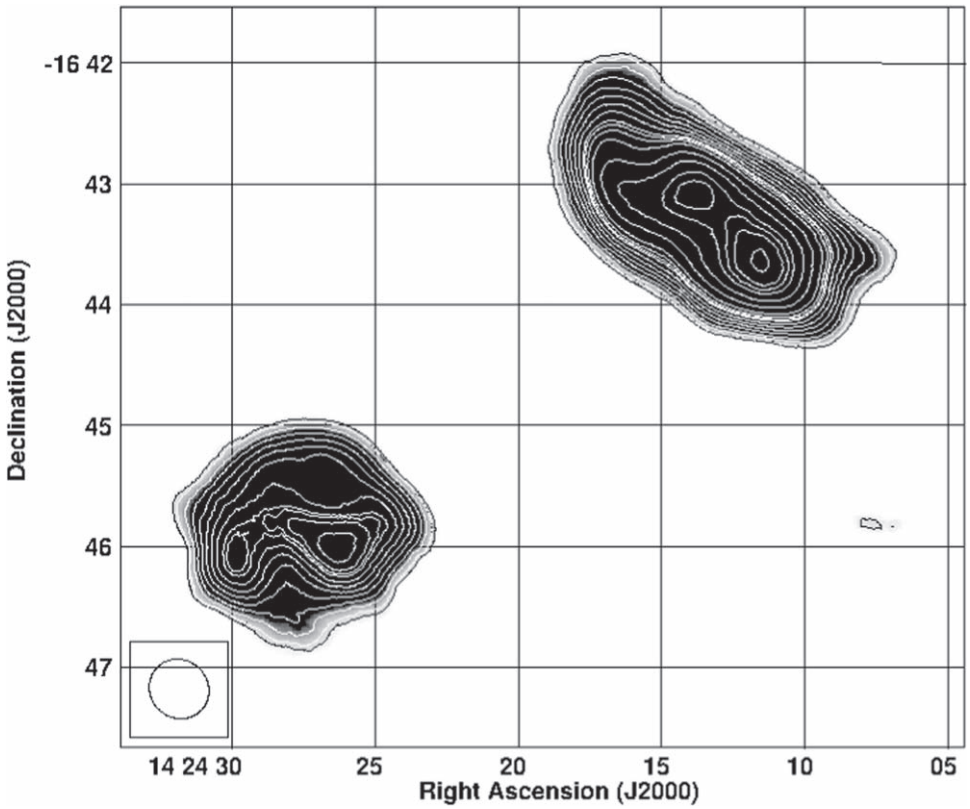

Figure 14. Our low-resolution VLA B-configuration H I 21 cm moment 0 image in gray scale and contours, obtained using a *uv* range restricted between zero and 5 kλ to search for any H I 21 cm intergalactic extended emission or bridges associated with the disks of NGC 5595 and NGC 5597. Here NGC 5597 is at the SE, and NGC 5595 is at the NW. The gray-scale stretch is 250–450 mJy beam^{-1} km s^{-1}. The moment 0 contours are at 15, 17, 21, 25, 30, 35, 40, 45, 50, 52, 55, 60, 70, 80, 90, 95, 100, and 108 $\times$ 1σ, where 1$\sigma \sim$ 19.45 mJy beam^{-1} km s^{-1}. No intergalactic H I 21 cm structure or filaments exist between the two galaxies. The synthesized beam at FWHM, which is $\sim$30.″7 $\times$ 28.″8 at P.A. $\sim$ +50° E of N, is shown in the bottom left corner.

(Yun et al. 1994), and the long tidal tails of the Antennae system NGC 4038/9 (van der Hulst 1979; Gordon et al. 2001; Hibbard et al. 2001). Computer *N*-body simulations have well reproduced the stellar and H I (21 cm) long tidal tails of the Antennae system (Barnes 1998). However, despite much effort, no satisfying model is yet available to reproduce the long SE H I 21 cm tidal tail in the M51 system (Toomre 1978; Hernquist 1990; Barnes 1998).

7. Summary and Conclusions

In this study, we have obtained VLA B-configuration H I 21 cm kinematical data from the close pair disk galaxies NGC 5597 SBc(s) and NGC 5595 Sc(s). We have detected for the first time the existence of cold atomic hydrogen H I 21 cm extended structures (streamers) to the NE and SW of NGC 5595 with no blue or red optical continuum or 20 cm radio continuum counterparts. They may be filamentary features as a result of recent gravitational tidal interaction with the neighbor NGC 5597 to the SE.

We were able to get the best-fit velocity fields, rotation curves (V versus R), and angular velocities ($\Omega_{\rm gas}$ versus R) for both disk galaxies, NGC 5595 and NGC 5597, from their heliocentric H I 21 cm recession velocities, assuming that the gas is in circular orbits around the nucleus. We have presented the H I 21 cm spectra for NGC 5597 and NGC 5595 and estimated the H I 21 cm gas mass from many clouds in both NGC 5595 and NGC 5597, as well as the total H I 21 cm gas mass in both galaxies.

Our H I 21 cm fitted parameters indicate that the disk rotation axis in NGC 5597 projected on the plane of the sky is at P.A. $\sim$ 190 E of N pointing in the SW direction; thus, the hemisphere from NW clockwise toward SE is closer to the observer. The disk rotation axis in NGC 5595 projected on the plane of the sky is at P.A. $\sim$ 327 E of N pointing in the NW direction; thus, the NE hemisphere clockwise toward SW is closer to the observer.

We have also presented new 20 cm radio continuum emission images from both NGC 5595 and NGC 5597. In particular, in NGC 5597, our image shows an unresolved central emission peak with an elongated structure that coincides with previously published Hα+N[II] line emission. Both emissions come from the innermost central region, where there is no cold hydrogen atomic gas in NGC 5597. The existence of Hα and 20 cm radio continuum and the lack of H I 21 cm at the center of NGC 5597 are very similar to the distribution observed in other nearby barred galaxies and might suggest a central SMBH with a mass of a few $\times$ 10^6 $M_\odot$.

Finally, we have made low-resolution ($\approx$30″ at FWHM) H I 21 cm images of the field of the pair disk galaxy system NGC 5595 and NGC 5597 and did not detect any extended intergalactic H I 21 cm tails or bridges between the disk galaxies.

We thank the anonymous referee for suggestions and comments that have significantly enhanced the content of this manuscript.

Facility: EVLA.

Software: AIPS (Greisen 2003), CASA (McMullin et al. 2007).

ORCID iDs

J. Antonio Garcia-Barreto https://orcid.org/0000-0002-3773-9613
Emmanuel Momjian https://orcid.org/0000-0003-3168-5922

References

Appleton, P. N., Foster, P. A., & Davies, R. D. 1986, MNRAS, 221, 393
Argudo-Fernande3z, M., Verley, S., Bergond, G., et al. 2015, A&A, 578, A110
Athanassoula, E. 1992, MNRAS, 259, 345
Barnes, J. 1990, in N-body Studies of Major Mergers in Dynamics and Interactions of Galaxies, ed. R. Wielen (Berlin: Springer), 186
Barnes, J. 1998, in Galaxies: Interactions and Induced Star Formation, ed. D. Friedli, L. Martinet, & D. Pfeniger (Berlin: Springer), 275
Binney, J., & Tremaine, S. 1987, Galactic Dynamics (Princeton, NJ: Princeton Univ. Press)
Burton, W. B. 1974, Galactic and Extragalactic Radio Astronomy (New York: Springer), 92
Cecil, G. 1988, ApJ, 329, 38
Combes, F., Boissé, P., Mazure, A., & Blanchard, A. 2002, Galaxies and Cosmology (Berlin: Springer)
Condon, J. J., Helou, G., Sanders, D. B., & Soifer, B. T. 1990, ApJS, 73, 359
Contopoulos, G. 1988, A&A, 201, 44
Contopoulos, G., Gottesman, S. T., Hunter, J. H., Jr., & England, M. N. 1989, ApJ, 343, 608
Cottrell, G. A. 1976, MNRAS, 174, 455
Crane, P., & van der Hulst, J. 1992, AJ, 103, 1146
Davies, R. D. 1974, in IAU Symp. 58, The Formation and Dynamics of Galaxies, ed. J. R. Shakeshaft (Dordrecht: Reidel), 119
de Vaucouleurs, G., de Vaucouleurs, A., Corwin, H. G., et al. 1993, Third Reference Catalog of Galaxies (New York: Springer), RC3
Diaz-Hernández, R., Garcia-Barreto, J. A., & Moreno-Corral, M. A. 2009, RMxF, E55, 70
England, M. N. 1989, ApJ, 337, 191
Field, G. F. 1958, I.R.E., 16, 240
Field, G. F. 1959, ApJ, 129, 536
Ford, H. C., Crane, P. C., Jacoby, G. H., Lawrie, D. G., & van der Hulst, J. M. 1985, ApJ, 293, 132
Garcia-Barreto, J. A., Carrillo, R., & Vera-Villamizar, N. 2003, AJ, 126, 1707
Garcia-Barreto, J. A., Combes, F., Koribalski, B., & Franco, J. 1999, A&A, 348, 685
Garcia-Barreto, J. A., Franco, F., Carrillo, R., Venegas, S., & Escalante-Ramirez, B. 1996, RMxAA, 32, 89
Garcia-Barreto, J. A., Franco, J., & Rudnick, L. 2002, AJ, 123, 1913
Garcia-Barreto, J. A., Mayya, D. Y., & Guichard, J. 2019, PASP, 131, 094101
Garcia-Barreto, J. A., & Momjian, E. 2022, AJ, 164, 91
Garcia-Barreto, J. A., & Moreno, E. 2000, ApJ, 529, 832
Garcia-Barreto, J. A., Rudnick, L., Franco, F., & Martos, M. 1998, AJ, 116, 111
Garcia-Barreto, J. A., Scoville, N. Z., Koda, J., & Sheth, K. 2005, AJ, 129, 125
Gebhardt, K., Bender, R., & Bower, G. 2000, ApJL, 539, L13
Geller, M., Kenyon, S. J., Baros, E. J., Jarnett, T. H., & Kewley, L. J. 2006, AJ, 132, 2243
Goad, J. W. 1976, ApJS, 32, 89
Gordon, S., Koribalski, B., & Jones, K. 2001, MNRAS, 326, 578
Greisen, E. W. 2003, Information Handling in Astronomy—Historical Vistas, Vol. 285 (Dordrecht: Kluwer), 109
Haan, S., Schinnerer, E., Mundell, C. G., Garcia-Burillo, S., & Combes, F. 2008, AJ, 135, 232
Haynes, M., Giovanelli, R., & Burkhead, M. S. 1978, AJ, 83, 938
Helou, G., Soifer, B. T., & Rowan-Robinson, M. 1985, ApJL, 298, L7
Hernández-Toledo, H. M., Cano-Diaz, M., Valenzuela, O., et al. 2011, AJ, 142, 182
Hernquist, L. 1990, in Dynamicas and Interaction of Galaxies, ed. R. Wielen (Berlin: Springer), 108
Hibbard, J. E., van der Hulst, J. M., Barnes, J. E., & Rich, R. M. 2001, AJ, 122, 2969
Ho, L. C., Greene, J. E., Filippenko, A. V., & Sargent, W. L. 2009, ApJS, 183, 1
Ho, L. C., & Ulvestad, J. S. 2001, ApJS, 133, 77
Hummel, E. 1981, A&A, 96, 111
Hummel, E., van der Hulst, J. M., Keel, W. C., & Kennicutt, R. C., Jr. 1987, A&AS, 70, 517
Hummel, E., van der Hulst, J. M., Kennicutt, R. C., Jr., & Keel, W. C. 1990, A&A, 236, 333
Karachentsev, I. D. 1972, Commn.Special Astrophys. Obs. USSR, 7, 1
Karachentsev, I. D. 1981, Ap, 17, 135
Linde, S. T., & Mihos, J. C. 2022, ApJL, 933, L33
Mathewson, D. S., Ford, V. L., & Buchhorn, M. 1992, ApJS, 81, 413
McMullin, J. P., Water, B., Schiebel, D., Yound, W., & Golap, K. 2007, in ASP Conf. Ser. 376, Astronomical Data Analysis Software and Systems, XVI, ed. R. A. Shaw, F. Hill, & D. J. Bell (San Francisco, CA: ASP), 127
Merritt, D., & Ferrarese, L. 2001a, ApJ, 547, 140
Merritt, D., & Ferrarese, L. 2001b, MNRAS, 320, L30
Mihalas, D., & Binney, J. 1981, Galactic Astronomy (2nd edn.; San Francisco, CA: Freeman)
Mihos, J. C., & Hernquist, L. 1994, ApJL, 425, L13
Mihos, J. C., & Hernquist, L. 1996, ApJ, 464, 641
Moody, J. W., Roming, P. W. A., Joner, M. D., et al. 1995, AJ, 110, 2088
Norman, G., & Silk, J. 1983, ApJ, 266, 502
Paturel, G., Thereau, G., Bottinelli, L., et al. 2003, A&A, 412, 57
Planesas, P., Scoville, N. Z., & Myers, S. T. 1991, ApJ, 369, 364
Purcell, E. M., & Field, G. B. 1956, ApJ, 126, 542
Reid, M. J., Biretta, J. A., Junor, W., Muxlow, T. W. B., & Spencer, R. E. 1989, ApJ, 336, 112
Rogstad, D. H., Lockhart, I. A., & Wright, M. C. H. 1974, ApJ, 193, 309
Rots, A. H., Bosma, A., van der Hulst, J. M., Athanassoula, E., & Crane, P. C. 1990, AJ, 100, 387
Sancisi, R. 1999, in IAU 186 Galaxy Interactions at Low and High Redshifts, ed. J. E. Barnes & D. B. Sanders (Dordrecht: Kluwer), 71
Sandage, A., & Tammann, G. A. 1981, A Revised Shapley-Ames Catalog of Bright Galaxies (Washington, DC: Carnegie Institution of Washington Publ.), 635
Scoville, N. Z. 1988, Galactic and Extragalactic Star Formation, 232 (Dordrecht: Kluwer), 541
Scoville, N. Z., Yun, M. S., Armus, L., & Ford, H. 1998, ApJL, 493, L63
Spitzer, L., Jr. 1978, Physical Processes in the Interstellar Medium (New York: Wiley)
Springob, C. M., Haynes, M. P., Giovanelli, R., & Kent, B. R. 2005, ApJS, 160, 149
Stocke, J. T. 1978, AJ, 83, 348
Stocke, J. T., Tifft, W. G., & Kaftan-Kassim, M. A. 1978, AJ, 83, 322
Tammann, G. A. 1985, in Conf. Proc. 20, The Virgo Cluster of Galaxies, ed. O.-G. Richter & B. Binggeli (Garching: ESO), 3
Toomre, A. 1978, in Interacting Systems in IAU 79 The Large Scale Structure of the Universe, ed. M. S. Longair & J. Einasto (Dordrecht: Reidel), 109
Toomre, A. 1983, in Theories of Warps in Internal Kinematics and Dynamics of Galaxies, ed. E. Athanassoula (Dordrecht: Kluwer), 177
Toomre, A., & Toomre, J. 1972, ApJ, 178, 623
Tully, R. B. 1988, Nearby Galaxies Catalog (Cambridge: Cambridge Univ. Press)
Tully, R. B., & Fischer, J. R. 1987, Nearby Galaxies Atlas (Cambridge: Cambridge Univ. Press)
Ulvestad, J. S., Neff, S. G., & Wilson, A. S. 1987, AJ, 93, 22
van der Hulst, J. M. 1979, A&A, 75, 97
van der Hulst, J. M., Hummel, E., & Dickey, J. M. 1982, ApJL, 261, L59
Veilleux, S., Cecil, G., Bland-Hawthorn, J., et al. 1994, ApJ, 433, 48
Wilson, A. S., & Ulvestad, J. S. 1987, ApJ, 319, 105
Woods, D. F., & Geller, M. 2007, AJ, 134, 527
Wright, M. C. H. 1974, Mapping Neutral Hydrogen in External Galaxies in Galactic and Extragalactic Radio Astronomy (New York: Springer)
Yun, M. S., Ho, P. T. P., & Lo, K. Y. 1993, ApJL, 411, L17
Yun, M. S., Ho, P. T. P., & Lo, K. Y. 1994, Natur, 372, 530
Zwicky, F. 1956, ErNW, 29, 344